

2009

Neisseria gonorrhoeae PriB: a probe to the mechanisms of bacterial DNA replication restart pathways

Jinlan Dong
University of Dayton

Follow this and additional works at: https://ecommons.udayton.edu/graduate_theses

Recommended Citation

Dong, Jinlan, "Neisseria gonorrhoeae PriB: a probe to the mechanisms of bacterial DNA replication restart pathways" (2009). *Graduate Theses and Dissertations*. 2387.
https://ecommons.udayton.edu/graduate_theses/2387

This Thesis is brought to you for free and open access by the Theses and Dissertations at eCommons. It has been accepted for inclusion in Graduate Theses and Dissertations by an authorized administrator of eCommons. For more information, please contact mschlange1@udayton.edu, ecommons@udayton.edu.

***Neisseria gonorrhoeae* PriB: A Probe to the Mechanisms of Bacterial
DNA Replication Restart Pathways**

Thesis

Submitted to

The College of Arts and Sciences of the

UNIVERSITY OF DAYTON

In Partial Fulfillment of the requirements for

The Degree

Master of Science in Chemistry

By

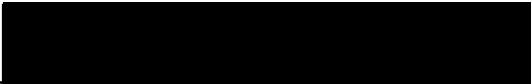
Jinlan Dong

UNIVERSITY OF DAYTON

Dayton, Ohio

December, 2009

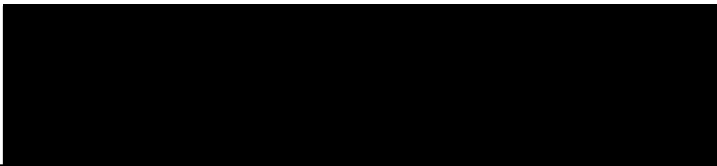
APPROVED BY:



Matthew E. Lopper, Ph.D.
Assistant Professor
Department of Chemistry
University of Dayton
Faculty Advisor



R. Gerald Keil, Ph.D.
Professor
Department of Chemistry
University of Dayton



Kevin M. Church, Ph.D.
Associate Professor
Department of Chemistry
University of Dayton

ABSTRACT

***Neisseria gonorrhoeae* PriB: A Probe to the Mechanisms of Bacterial DNA Replication Restart Pathways**

**Name: Dong, Jinlan
University of Dayton**

Advisor: Dr. Matthew E. Lopper, Ph.D.

DNA is a marvelous storage device for genetic information, and its complete and faithful duplication is essential for the propagation of life. However, the integrity of DNA is often marred by DNA damage arising from the environment or from cellular metabolism. Regardless of the source, DNA damage can disturb processes that read and copy the genetic information. In order to survive, cells must be able to resume the process of DNA replication following encounters of the replication machinery with damaged DNA. In bacteria, this process is known as DNA replication restart and it involves a set of proteins called primosome proteins. *Neisseria gonorrhoeae*, a medically important bacterium, is heavily dependent on DNA replication restart pathways to survive in host cells. Here, we describe a high-resolution crystal structure of a *Neisseria gonorrhoeae* DNA replication restart primosome protein called PriB. PriB is a homodimer that is comprised of a single structural domain consisting of two oligosaccharide/oligonucleotide binding (OB) folds. PriB is a

single-stranded DNA-binding protein that binds single-stranded DNA via the classic ligand binding surface of its OB folds. Furthermore, PriB has a direct and robust physical interaction with another primosome protein called PriA helicase. The high affinity of *Neisseria gonorrhoeae* PriA and PriB lies in stark contrast to the low affinity interaction observed between *E. coli* PriA and PriB proteins and might represent a way in which the DNA replication restart machinery of *Neisseria gonorrhoeae* has become specialized to help *Neisseria gonorrhoeae* cells respond to oxidative damage to their DNA.

ACKNOWLEDGEMENTS

My special thanks are in order to Dr. Matthew E. Lopper, my research advisor, for giving me a great opportunity to do this research in his laboratory and guiding me through. Besides his numerous help on my research, Dr. Lopper helped me a lot for my future study. I appreciate his understanding and support at all times and I am honored to do my graduate research with him.

I would like to express my appreciation to every one who helped me with my study and work in University of Dayton. This includes my undergraduate co-worker Katrina Duckett who also worked on *N. gonorrhoeae* PriB, my committee member Dr. Gerald Keil and Dr. Kevin M. Church who gave me valuable advices on my research, Dr. Mark Masthay for the UV-spectrophotometer in his lab, and Nicholas George (University of Wisconsin-Madison) who collected X-ray data for us at the Argonne National Laboratories. In addition, I want to say thank you to Dr. David Johnson, Dr. Gary Morrow, Dr. Shawn Swavey and Dr. Vladimir Benin whose classes I learned a lot from. Special thanks go to Dr. Kimberly Trick and Paula Keil for their valuable help with my teaching, Mark Sidenstick and Gary Miller for their suggestion on my teaching, and Judy Scheidt and Connie Schell for their kind help with my work. They all make my two years of study at University of Dayton unforgettable. I would also like to thank the

chemistry department for supporting my study and research at University of Dayton and graduate school for the graduate summer fellowships which supported my summer research in summer 2008 and summer 2009.

Last but not least, this work is dedicated to my parents, my brother, and my friends, for their love and support under all circumstances!

TABLE OF CONTENTS

ABSTRACT.....	iii
ACKNOWLEDGEMENTS.....	v
CHAPTER I INTRODUCTION.....	1
CHAPTER II EXPERIMENTAL METHODS.....	10
II-1 Site-directed mutagenesis.....	10
II-2 Purification of <i>N. gonorrhoeae</i> PriA.....	11
II-3 Purification of <i>N. gonorrhoeae</i> PriB variants.....	14
II-4 Florescein isothiocyanate(FITC)-labeling <i>N. gonorrhoeae</i> PriB.....	17
II-4-1 FITC-labeling wild-type <i>N. gonorrhoeae</i> PriB.....	17
II-4-2 FITC-Labeling of PriB Variants (K34A, K81A, Y21A and E41A).....	19
II-5 Fluorescence polarization spectroscopy.....	21
II-6 Affinity Pull-down experiments.....	25
II-7 Crystallization of PriB: single-stranded DNA complexes.....	28
CHAPTER III RESULTS AND DISCUSSION.....	34
III-1 <i>N. gonorrhoeae</i> PriB is a single-stranded DNA-binding protein.....	34
III-2 Identification of PriB's Binding site for ssDNA.....	36
III-3 <i>N. gonorrhoeae</i> PriB physically interacts with <i>N. gonorrhoeae</i> PriA.....	41
III-4-1 Identification of PriB's binding sites for PriA using affinity pull-down experiments.....	44
III-4-2 Identification of PriB's binding sites for PriA using FP experiments.....	47
CHAPTER IV CONCLUSIONS AND FUTURE DIRECTION.....	50
IV-1 Conclusions.....	50
IV-2 Future Direction.....	51
REFERENCES.....	52
APPENDICES.....	57
A-1 EXPRESSION OF <i>E. coli</i> DnaB.....	58
A-2 PURIFICATION OF <i>E. coli</i> DnaB.....	60
A-3 BINDING ABILITY OF <i>E. coli</i> DnaB.....	66
A-3-1 Interaction between <i>E. coli</i> DnaB and FITC-DnaT.....	66
A-3-2 Interaction between <i>E. coli</i> DnaB and FITC-PriB.....	67
A-4 EXPRESSION OF <i>E. coli</i> DnaC.....	69

LIST OF FIGURES

Figure 1. DNA replication restart allows complete and faithful duplication of bacterial genome.....	3
Figure 2. Replisome loading systems in <i>E.coli</i>	4
Figure 3. An inducible recombinant protein overexpression system.....	11
Figure 4. Purification of <i>N.gonorrhoeae</i> PriA.....	13
Figure 5. Purification of <i>N.gonorrhoeae</i> PriB and its variants.....	16
Figure 6. Schematic layout of the general L-format fluorescence polarization spectroscopy equipment	23
Figure 7. Fluorescence anisotropy facilitates detection of macromolecule Interactions.....	24
Figure 8. Idealized gel electrophoresis analysis of protein:protein interactions using an affinity pull-down experiment.....	26
Figure 9. The workflow of an affinity pull-down experiment.....	27
Figure 10. X-ray diffraction pattern of a protein crystal.....	30
Figure 11. Workflow for solving the structure of a molecule by X-ray crystallography.	32
Figure 12. Diagram of hanging-drop vapor diffusion method.....	32
Figure 13. Orthogonal views of the crystal structures of <i>N.gonorrhoeae</i> PriB and <i>E.coli</i> PriB.....	35
Figure 14. Crystals of <i>N.gonorrhoeae</i> PriB growth in the absence (left) and presence (right) of ssDNA.....	36
Figure 15. Locations of substituted amino acid residues.....	37
Figure 16. <i>N.gonorrhoeae</i> PriB variants have altered ssDNA binding activities.....	38
Figure 17. <i>N.gonorrhoeae</i> PriB and <i>E.coli</i> PriB differ in their ssDNA binding activity and surface charge properties.....	40
Figure 18. <i>N.gonorrhoeae</i> PriA and PriB form a complex that is species specific.....	43
Figure 19. Affinity pull-down experiments with <i>N. gonorrhoeae</i> PriA and PriB.....	45
Figure 20. <i>N.gonorrhoeae</i> PriB variants were pulled down by PriA except E41A and K81A.....	46
Figure 21. Variation of surface residues of PriB homologs.....	48

Figure 22. Timecourse of DnaB overexpression in <i>E.coli</i> cells.....	59
Figure 23. Purification process of <i>E. coli</i> DnaB.....	62
Figure 24. Results of DnaB purification process.....	64
Figure 25. Overexpression of DnaC in LB/Kan medium.....	71
Figure 26. Overexpression of DnaC in 2YT/Kan medium.....	72
Figure 27. Overexpression of DnaC in the presence of glucose.....	73

CHAPTER I

INTRODUCTION

Deoxyribonucleic acid (DNA) occupies a unique and central place among biological macromolecules. The nucleotide sequences of DNA encode the information needed to encode the primary structures of all cellular RNAs and proteins, and, through enzymes, indirectly affect the synthesis of all other cellular constituents¹. DNA replication, the process of reading and copying the genetic information in DNA, represents one of the central pathways in genome maintenance and is essential for cellular growth and division. In many organisms, remarkably efficient mechanisms have evolved to coordinate and regulate DNA replication. The enzymes that synthesize DNA, collectively called the replisome, copy DNA molecules with extraordinary fidelity and speed. For example, the replication machinery of *E. coli* cells is capable of synthesizing new DNA at a replication fork at a rate of approximately 1,000 nucleotides per second with remarkable fidelity².

However, the DNA genome is an imperfect template. DNA damage arising from the environment or from cellular metabolism creates physical barriers that disrupt the reading and copying of genetic information from the DNA template. As a result, DNA replication is particularly sensitive to DNA

damage since advancing replisomes can derail upon encountering the vast arrays of DNA lesions that can occur in cells, including single-stranded DNA (ssDNA) nicks and gaps, double-stranded DNA breaks, and chemically modified bases^{3,4}. These types of DNA damage can permanently affect or eliminate the function of a gene and can affect how the DNA is duplicated by interfering with the enzymes that replicate DNA.

To ensure complete and faithful replication of the genome, it is not surprising that cells have evolved mechanisms to overcome the obstacles posed by the imperfections in the template DNA. In bacterial cells, this process is called DNA replication restart (Figure 1). Cells use this pathway to overcome the barriers posed by DNA damage and rescue disrupted replisomes so that DNA replication can proceed to completion. In bacteria, primosome proteins function to rescue DNA replication following encounters of the replication machinery with DNA damage, although the mechanisms by which they function are not entirely understood.

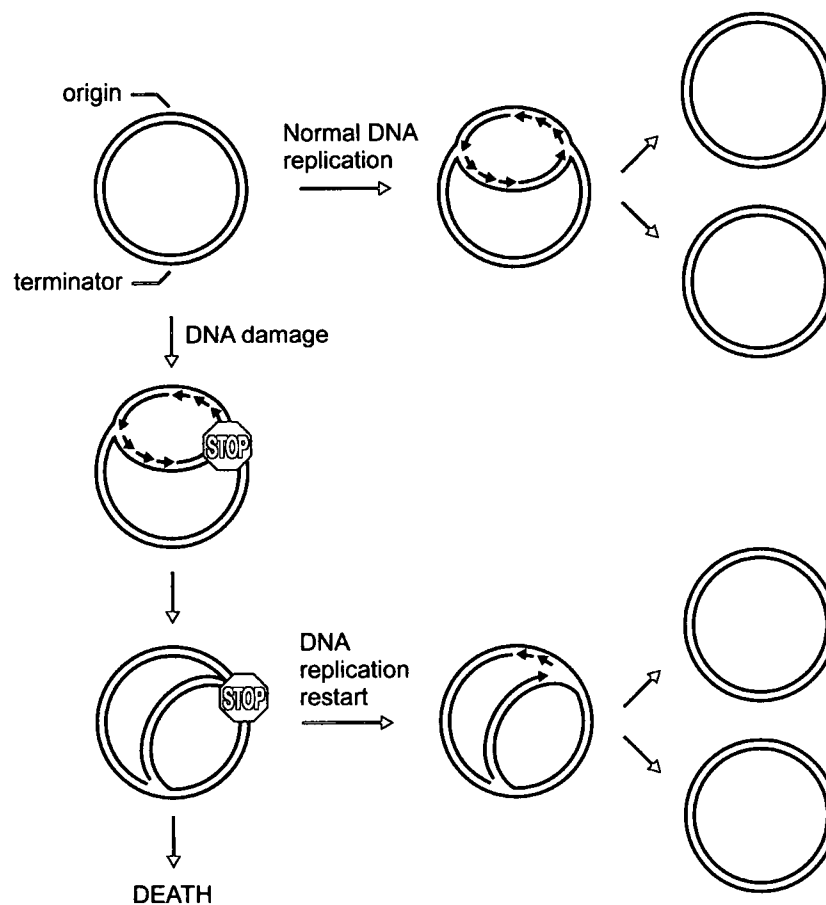
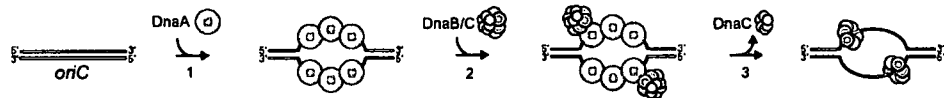


Figure1. DNA replication restart allows complete and faithful duplication of bacterial genome. DNA duplication normally initiates at an origin of replication and ends at terminator sequences. When replisomes encounter DNA damage, DNA replication can be disrupted, leading to cell death. DNA replication restart facilitates complete and faithful duplication of the genome, allowing cells to survive and grow.

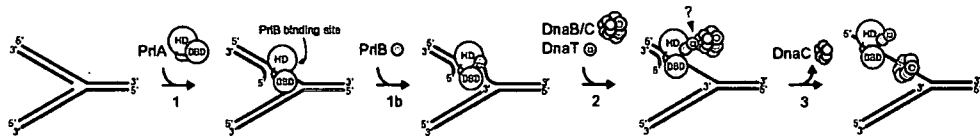
In *E. coli* cells, initiation of DNA replication at an origin of replication is a carefully regulated, sequence-specific event that involves the activity of an initiator protein called DnaA. DnaA unwinds the duplex DNA at the origin (Figure 2A, step 1), producing the single-stranded DNA necessary for the

recruitment of the replicative helicase (DnaB) and its associated loading factor (DnaC) (Figure 2A, step 2), followed by loading of DnaB onto the DNA (Figure 2A, step 3). After loading DnaB, DNA synthesis enzymes are recruited to complete DNA replication. The DNA structure that is formed by DnaB is called a replication fork and it has two branches called the leading and lagging strands.

A. DnaA system



B. PriA-PriB-DnaT system



C. PriC system

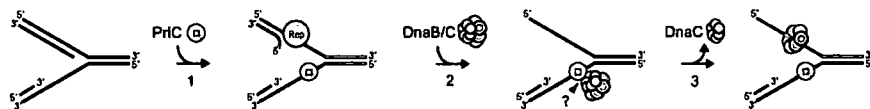


Figure 2. Replisome loading systems in *E. coli*. A) Origin-dependent replisome loading. DnaA protein binds the origin, *oriC*, and unwinds duplex DNA to allow loading of DnaB from the DnaB/C complex. B) Origin-independent replisome loading. PriA binds a repaired replication fork with no leading strand gap, unwinds the lagging strand arm, and recruits PriB and DnaT. The PriA-PriB-DnaT complex recruits DnaB through an unknown mechanism. C) Origin-independent replisome loading. PriC binds a repaired replication fork with a leading strand gap and recruits DnaB through an unknown mechanism. Since replication forks can encounter DNA damage at

sites far removed from an origin, cells require an alternative means of reinitiating DNA replication at non-origin sequences where a replication fork has been disrupted. The proteins that are responsible for this activity are collectively known as the DNA replication restart primosome and include PriA, PriB, PriC, DnaT, and Rep proteins. While the ultimate goal of DNA replication restart pathways is similar to initiation of DNA replication at an origin, DNA replication restart pathways need a distinct mechanism from origin-dependent replisome loading. In contrast to sequence-specific initiation of DNA replication at the origin, DNA replication restart initiator proteins bind to specific DNA structures that form as a result of DNA recombination or repair pathways.

Genetic lines of investigation in *E. coli* led to the "multiple replication restart pathways" model, stemming from observations that non-functional mutations in *priA*, *priB*, *priC*, and *dnaT* genes do not all display identical cellular phenotypes as would be expected for genes that operate in a single pathways^{5,6}. Now, two distinct replisome loading systems have been biochemically defined, one requiring PriA, PriB, and DnaT, and the other one requiring only PriC⁷. The primary difference between these two mechanisms appears to be their preference for specific DNA structures: PriA operates on forks with no leading strand gap at the three-way junction, while PriC prefers forks with a gap (Figure 2 B, C).

In the well-studied bacterial model organism, *E. coli*, the ability to reactivate repaired DNA replication forks is essential for genome maintenance and cell survival. Given the broad conservation of key DNA replication restart

primosome genes (for example, *priA* is encoded in 1111 out of 1289 sequenced bacterial chromosomes), little is known about DNA replication restart in other organisms. But it is likely that the importance of DNA replication restart pathways extends throughout much of the bacterial world. Therefore, I chose to examine DNA replication in *Neisseria gonorrhoeae*, a bacterium that relies heavily on DNA replication restart pathways for its growth and survival.

Neisseria gonorrhoeae is the causative agent of gonorrhea. The hallmark of acute *N. gonorrhoeae* infection is a purulent discharge consisting of neutrophils, which are associated with the inflammatory response mounted against the *N. gonorrhoeae* infection⁸. Neutrophils perpetrate an oxygen-dependent bactericidal attack with the release of numerous highly reactive compounds, including superoxide and H₂O₂, resulting in DNA and protein damage in the microbe. *N. gonorrhoeae* may also encounter H₂O₂ produced by commensal organisms often associated with *N. gonorrhoeae* in vivo⁹. *N. gonorrhoeae* is highly adapted to survive oxidative damage, as evidenced by their ability to survive within and among neutrophils^{8, 10}. In addition, since *N. gonorrhoeae* is an obligate human pathogen and is unlikely to be subject to damage by chemical and physical agents in the environment (e.g., UV and ionizing radiation, chemical mutagens, desiccation), it is probable that a major source of DNA damage stems from free radicals endogenously generated during aerobic respiration¹¹. Consistent with this is the fact that *N. gonorrhoeae* cells possess a number of defenses to counteract oxidative damage, including catalase¹², cytochrome c oxidase¹³ and

cytochrome c peroxidase^{14,15}, peptide methionine sulfoxide reductase¹⁶, and a Mn-dependent superoxide quenching mechanism¹⁷.

To maintain genome integrity in the face of DNA damage, *N. gonorrhoeae* has developed various strategies to reverse, excise, or tolerate DNA damage products via a network of DNA repair mechanisms, including base excision repair, nucleotide excision repair, mismatch repair, and recombinational repair¹⁸. In *E. coli* cells, a primosome protein called PriA is central to the restart of chromosomal replication when replication fork progression is disrupted and is also involved in homologous recombination and DNA repair. This conclusion is supported by observations that PriA-mediated replication fork assembly can rescue arrested replication forks¹⁹, data showing that PriA binds D-loops with high specificity^{20,21}, and studies characterizing the genetic pathways of DNA replication restart²². The genome of *N. gonorrhoeae* encodes a homolog of PriA that seems to be important for DNA repair and DNA transformation²³. PriA mutants show a growth deficiency and decreased DNA repair capability and are completely deficient in DNA transformation compared to the isogenic parental strain. The PriA mutant is also more sensitive to H₂O₂²³ compared to the parental strain. These phenotypes are largely complemented by supplying a functional copy of *pria* elsewhere in the chromosome. Taken together, these data demonstrate that *N. gonorrhoeae* is heavily dependent on DNA replication restart pathways for survival and the primosome protein PriA plays an important role in the DNA replication restart process, although the details of this mechanism have not been understood completely.

In addition to PriA, the genome of *N. gonorrhoeae* encodes a homolog of PriB that is important for DNA replication restart in *E. coli* cells following encounters of the replication machinery with DNA damage. In *E. coli* cells, the PriA-dependent pathway is the major DNA replication restart mechanism that requires primosome proteins for replisome reloading where PriB plays an important role. In *E. coli* cells, structural analysis of *E. coli* PriB has revealed structural similarity between *E. coli* PriB and ssDNA binding proteins (SSBs)^{24,25,26}. The classic ligand binding surface of PriB's oligonucleotide/oligosaccharide binding (OB) folds mediates interactions with ssDNA, akin to SSBs^{25,28,29}. Besides, *E. coli* PriB can physically interact with *E. coli* PriA in a DNA-dependent manner. What's more, it is known that significant overlap exists among PriB binding sites for ssDNA and PriA²⁹, suggesting that PriA and ssDNA compete with one another for bindings sites on PriB.

Based on the study of *E. coli* PriB²⁹, I hypothesized that *N. gonorrhoeae* PriB is a ssDNA binding protein that physically interacts with *N. gonorrhoeae* PriA and has overlapping binding sites for PriA and ssDNA. To test this hypothesis, I used equilibrium DNA binding experiments to demonstrate that PriB binds ssDNA. A high-resolution crystal structure of PriB obtained by X-ray crystallography was used to guide site-directed mutagenesis experiments which, when coupled with equilibrium DNA binding experiments, revealed that PriB binds ssDNA via the classic ligand binding surface of its OB folds. Furthermore, I used affinity pull-down experiments and equilibrium binding experiments to demonstrate that PriB has a direct and robust physical interaction with *N. gonorrhoeae* PriA. The high affinity interaction between *N.*

gonorrhoeae PriA and PriB lies in stark contrast to the low affinity interaction observed between *E. coli* PriA and PriB proteins and might represent a way in which the DNA replication restart machinery of *Neisseria gonorrhoeae* has become specialized to help *Neisseria gonorrhoeae* cells respond to oxidative damage to their DNA.

CHAPTER II

EXPERIMENTAL METHODS

II-I Site-directed mutagenesis

Mutagenesis was carried out on a pET28b:(*N. gonorrhoeae*) PriB template by PCR using the QuikChange II Site-Directed Mutagenesis Kit (Stratagene), as directed by the manufacturer. This method utilizes a supercoiled double-stranded DNA (dsDNA) vector with an insert of interest and two synthetic oligonucleotide primers, both containing the desired mutation. The oligonucleotide primers, each complementary to opposite strands of the vector DNA, are extended during temperature cycling by *PfuUltra* DNA polymerase. Following the temperature cycling, the product was treated with *Dpn I*. The *Dpn I* endonuclease (target sequence: 5'-Gm⁶ ATC-3') is specific for methylated and hemimethylated DNA and is used to digest the parental DNA template and to select for mutation-containing newly synthesized DNA. The vector DNA was transformed into XL 1-Blue supercompetent cells and single colonies were selected, amplified, and tested for the presence of vector DNA with the desired mutation. From this method, I constructed four variants of the *N. gonorrhoeae prib* gene: E41A, Y21A, K81A and K34A.

II-2 Purification of *N. gonorrhoeae* PriA

BL21(DE3) *E. coli* cells transformed with pET28b:(*N. gonorrhoeae*)PriA were incubated at 37°C in Luria-Bertani medium supplemented with Kanamycin (LB/Kan medium) overnight. On the second day, the overnight culture was transferred into 1 L LB/Kan medium and incubated at 37°C. Protein expression was induced by the addition of 0.5 mM isopropyl β -D-thiogalactopyranoside (IPTG) at OD₆₀₀ of greater than 0.4. The cells were incubated for 4 more hours before harvesting by centrifugation for 25 min at 5500 x g at 4°C. The cells were stored at -80°C

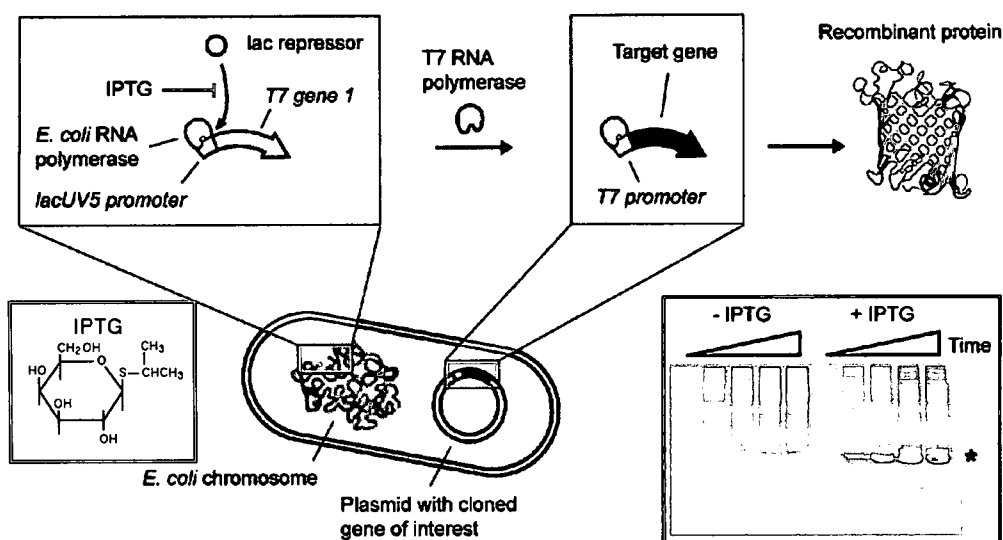


Figure 3. An inducible recombinant protein overexpression system.

IPTG induces *E. coli* cells to overexpress T7 RNA polymerase which increases the efficiency by which *E. coli* cells express protein encoded in the target gene in the inserted plasmid. IPTG is a highly stable synthetic analog of lactose and a particularly effective nonmetabolizable inducer of the *lac* operon. In *E. coli* cells, a gene of interest cloned into the plasmid will be transcribed when an

enzyme called T7 RNA polymerase binds to the T7 promoter just in front of the target gene in the plasmid. The enzyme T7 RNA polymerase is encoded in T7 gene 1 in the *E. coli* chromosome and is regulated by *lacUV5* promoter which is blocked by lac repressor normally. The work of IPTG is to remove the lac repressor from the promoter and turn on the transcription of T7 RNA polymerase to accelerate the transcription of the target gene. IPTG is an effective inducer as shown by comparison of protein overexpression levels in the presence and absence of IPTG (inset at lower right)

BL21(DE3) *E. coli* cells overexpressing *N. gonorrhoeae* PriA were thawed and suspended in Lysis Buffer [10 mM Hepes (pH 7.0), (v/v) 10% glycerol, 0.5M NaCl, 0.1 M glucose, 10mM imidazole, 1 mM phenylmethanesulphonylfluoride (PMSF) and 1 mM β -Mercaptoethanol (β -ME)] at a v/w ratio of 7 ml/gram cells. This process was followed by the addition of lysozyme to a final concentration of 200 μ g/mL. To decompose DNA and RNA, DNase I and RNase A were also added to a final concentration of 10 μ g/mL, and the mixture was sonicated. Insoluble debris was removed by centrifugation for 20 min at 40,000 x g at 4°C. Ni-NTA slurry was added to the supernatant and incubated for 1 hour at 4°C. The mixture was separated with a column. The beads binding with the desired recombinant protein were blocked and the waste was in the flow through. The beads were washed with one column volume Lysis Buffer and the protein was eluted by 15 mL Elution Buffer [10 mM Hepes (pH 7.0), (v/v) 10% glycerol, 100 mM NaCl, 200 mM imidazole, and 1 mM β -ME]. The elutant then was purified with an ion-exchange column equilibrated and washed with Buffer A [10 mM MES (pH 6.0), (v/v) 10% glycerol, 100 mM NaCl, and 1mM β -ME]. The protein

was eluted from the column with a linear gradient of Buffer B [10 mM MES (pH 6.0), (v/v) 10% glycerol, 1 M NaCl and 1mM β -ME]. The *N. gonorrhoeae* PriA-containing fractions, detected by 10% SDS-PAGE, were collected and concentrated overnight at 2600 x g and 4°C (Figure 4). The purified protein solution was stored at -80°C until use.

In every step, I collected 50 μ L samples for 1 SDS-PAGE analysis, which shows that the PriA solution has a purity of greater than 95% (Figure 4).

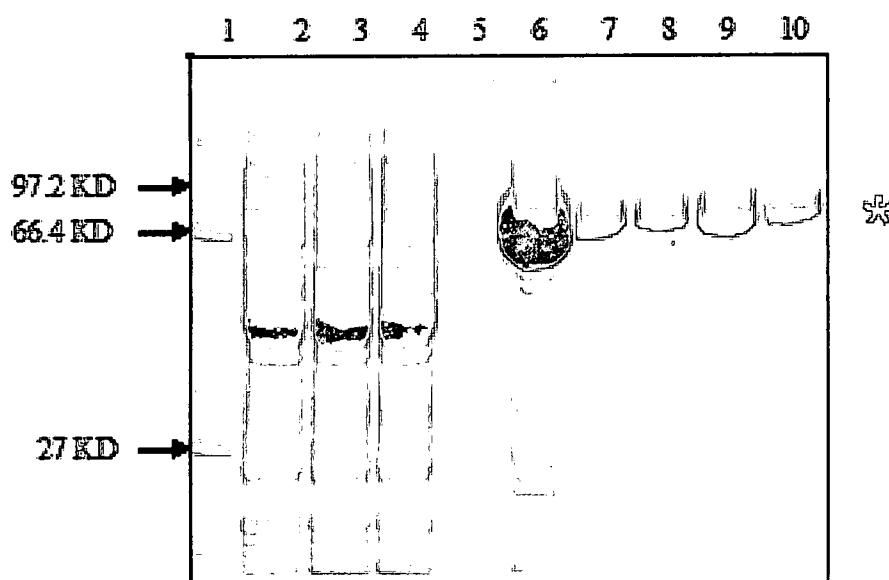


Figure 4. Purification of *N.gonorrhoeae* PriA. 1. protein marker; 2. crude lysate after sonication; 3. Ni column flow through; 4. early wash; 5. late wash; 6. elutant for Ni column; 7~10. *N.gonorrhoeae* PriA containing fractions from IEC. *N. gonorrhoeae* PriA has a molar mass 81.13 KD. It is in the position as the star shows.

II-3 Purification of *N. gonorrhoeae* PriB variants

Expression and purification of these four PriB variants and wild-type PriB followed the same steps, except that wild-type PriB was incubated in LB/Kan medium and the other four variants were incubated in LB/Kan/Chloramphenicol medium. BL21(DE3) cells transformed with pET28b:(*N. gonorrhoeae*) PriB and mutants were incubated at 37°C in the appropriate medium overnight. On the second day, the overnight culture was transferred into 1 L LB medium and incubated at 37°C. Protein expression was induced by the addition of 0.5 mM IPTG at an OD₆₀₀ of greater than 0.4. The cells were incubated for 4 more hours before harvest by centrifugation for 25 min at 4150 rpm at 4°C. The cells were stored at -80°C.

Cells individually overexpressing each *N. gonorrhoeae* PriB variant were suspended in Lysis Buffer [10 mM Tris-HCl (pH 8.5), (v/v) 10% glycerol, 100mM NaCl, 10 mM imidazole, 1 mM PMSF and 1 mM β-ME] at a v/w ratio of 7 ml/gram cells. This process was followed by the addition of lysozyme to a final concentration of 200 µg/mL. DNase I and RNase A were also added to a final concentration of 10µg/mL to decompose DNA and RNA, and the mixture was sonicated. Insoluble debris was removed by centrifugation for 20 min at 40,000 x g at 4°C. Ni-NTA agarose slurry was added to the supernatant and incubated for 1 hour at 4°C. The mixture was separated with a column. The beads were washed with three column volume Lysis Buffer and the protein was eluted by 15 mL Elution buffer [10 mM Tris-HCl (pH 8.5), (v/v) 10% glycerol, 100 mM NaCl, 250 mM imidazole, and 1 mM β-ME]. 200 units of thrombin was added to the protein solution and I dialyzed the suspension

against Dialysis Buffer [10 mM Tris-HCl (pH 8.5), (v/v) 10% glycerol, 100 mM NaCl and 1 mM β -ME] overnight at 4°C. This resulted in removal of the His-tag.

A second Nickel column was used after dialysis to get rid of the contaminating proteins. The mixture in the membrane tube was transferred into a 50 ml conical tube. 150 μ l 1M imidazole and 1 mL Ni-NTA slurry were added to it and the mixture was incubated at 4°C for an hour before it was transferred to a column to separate. This time, the flow through was collected to a Centriprep-YM-3 concentrator. The proteins solution was concentrated through centrifugation at 2600 x g at 4°C. After about an hour, when the volume of protein solution in the concentrator was about 6.5 mL, 0.4 M NaCl was added to it and I did not stop the concentration until the volume left in the concentrator was less than 2 mL. At this point, the concentrated protein was purified by size exclusion chromatography using a HiPrep 16/10 S100 column (GE Healthcare). The column was washed and equilibrated with S100 Buffer [10 mM Tris-HCl (pH 8.5), (v/v) 10% glycerol, 500 mM NaCl and 1 mM β -ME]. *N. gonorrhoeae* PriB- containing fractions, detected by 14% SDS-PAGE (Figure 5), were collected and concentrated at approximately 2600 x g overnight at 4°C. The concentration of protein solution was determined spectrophotometrically and the purified proteins were stored at -80°C until use.

Samples were also collected for each step in this protocol for SDS- PAGE analysis(Figure 5).

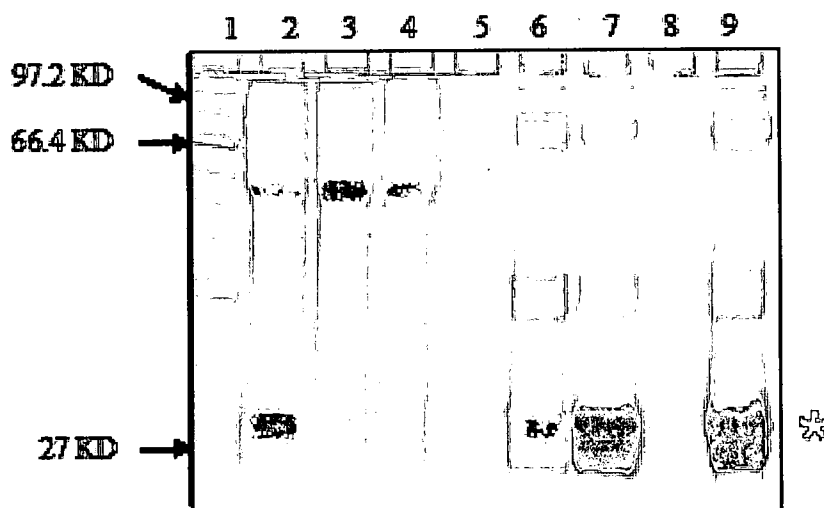


Figure 5. Purification of *N.gonorrhoeae* PriB and its variants. 1. protein marker; 2. crude lysate after sonication; 3. 1st Ni column flow through; 4. early wash of 1st Ni column; 5. late wash of 1st Ni column; 6. elutant for 1st Ni column; 7. after 2nd Ni column; 8. inner solution of the concentrator; 9. solution injected to S100 column. *N. gonorrhoeae* PriB has a molar mass 11.45 KD. It is in the position as the star shows.

For the PriB variant K81A, (v/v) 20% glycerol was used instead of (v/v) 10%. And I found that K81A variant had an extremely low solubility. When I added thrombin to the protein mixture and did the dialysis in Dialysis Buffer, some protein precipitated. In order to find a better buffer to increase its solubility, I tested in which buffer it has a higher solubility using its precipitate. Based on my test, I increased the concentration of glycerol to 20% in all the buffers to increase the solubility of K81A.

II-4 Florescein isothiocyanate(FITC)-labeling *N. gonorrhoeae* PriB

II-4-1 FITC-labeling wild-type *N. gonorrhoeae* PriB

Cells individually overexpressing each *N. gonorrhoeae* PriB variant were suspended in Lysis Buffer [10 mM Tris-HCl (pH 8.5), (v/v) 10% glycerol, 100 mM NaCl, 1 mM β -ME, 10 mM imidazole and 1 mM PMSF] at a v/w ratio of 7 ml/gram cells, which was followed by the addition of lysozyme to a final concentration of 200 μ g/mL. To decompose DNA and RNA, DNase I and RNase A were also added to a final concentration of 10 μ g/mL. And then the mixture was sonicated. Insoluble debris was removed by centrifugation for 20 min at 40,000 x g at 4°C. Ni-NTA slurry (4 ml/8L medium) was added to the supernatant and the mixture was incubated for 1 hour at 4°C, then was separated with a column. The beads blocked by the column were washed with three column volume of Lysis Buffer and the protein bound to the beads was eluted by 15 mL Elution Buffer [10 mM Tris-HCl (pH 8.5), (v/v) 10% glycerol, 100 mM NaCl, 250 mM imidazole, and 1 mM β -ME]. The elutant needed to be concentrated to a volume less than 2 ml before it was further purified by S100 column equilibrated and wasded with S100 Buffer [10mM Tris-HCl (pH 8.5), (v/v) 10% glycerol, 500 mM NaCl, and 1 mM β -ME]. After S100 column, I collected PriB containing fractions and extensively dialyzed the protein solution in a sodium bicarbonate buffer [0.1 M sodium bicarbonate (pH 9.0), 0.5M NaCl, 10% glycerol and 1mM β -ME] at 4°C.

The protein solution was incubated with a 20-fold molar excess of the amine-reactive dye called florescein isothiocyanate (FITC), dissolved in DMSO,

in the dark for an hour. The reaction was stopped by incubating the mixture of protein and dye with 0.1 ml 1 M Tris-HCl (pH 8.5) for 1 hour at room temperature. A second Nickel Column was used to harvest the labeled PriB. 4 ml Ni-NTA slurry was added to the bright yellow mixture and the mixture was incubated for 1 hour at room temperature. The mixture was transferred to a column and washed with 20 ml Wash Buffer [10 mM Tris-HCl (pH 8.5), (v/v) 10% glycerol, 100 mM NaCl, and 1 mM β -ME] until the flow through was clear and colorless and eluted by 10 ml elution buffer [10 mM, Tris-HCl (pH 8.5), (v/v) 10% glycerol, 100 mM NaCl, 1 mM β -ME and 500 mM imidazole]. 100 units of Thrombin was added to the elutant and the mixture was incubated overnight at 4°C.

In addition to the first two nickel columns, a third one was employed. I added 4 ml Ni-NTA slurry to the mixture solution and incubated them for 1 hour at 4°C. But this time, the flow through was collected to be dialyzed in 1 L S100 Buffer overnight. The dialyzed protein solution was concentrated and the concentration was measured by the UV-Spectrophotometer with wavelengths 280 nm and 494 nm and calculated as follows:

$$A_{\text{protein}} = A_{280} - A_{494} \text{ (CF)}$$

Where $CF = A_{280 \text{ free dye}} / A_{\text{max free dye}}$, for fluorescein isothiocyanate, $CF = 0.3$.

The concentration of protein was calculated assuming:

$$1.4 A_{\text{Protein}} = 1 \text{ mg/ml.}$$

In addition, the degree of labeling (D.O.L):

$$\text{D.O.L} = (A_{\text{max}} \times \text{MW}) / ([\text{protein}] \times \epsilon_{\text{dye}}), \epsilon_{\text{fluorescein}} = 68,000.$$

For FITC-*N.gonorrhoeae* PriB, A_{protein} is 1.6902, A_{494} is 0.2998, A_{protein} is 1.3904,

C_{protein} is 0.9931 mg/ml and D.O.L is 16.94%. The FITC-labeled PriB was stored at -80°C.

II-4-2 FITC-Labeling of PriB Variants (K34A, K81A, Y21A and E41A)

I suspended cells in Lysis Buffer [10 mM Tris-HCl (pH 8.5), (v/v) 20% glycerol, 100 mM NaCl, 1 mM β -ME, 10 mM imidazole and 1 mM PMSF] at a v/w ratio of 7 ml/gram cells, which was followed by the addition of lysozyme to a final concentration of 200 μ g/mL. To decompose DNA and RNA, DNase I and RNase A were also added to a final concentration of 10 μ g/mL before the mixture was sonicated. Insoluble debris was removed by centrifugation for 20 min at 40,000 x g at 4°C. Ni-NTA slurry was added to the supernatant and the mixture was incubated for 1 hour at 4°C, and then was separated with a column. The beads blocked by the column were washed with 1 column volume of Lysis Buffer and then the protein bound to the beads was eluted by 2 ml Elution Buffer [10 mM Tris-HCl (pH 8.5), (v/v) 20% glycerol, 100 mM NaCl, 500 mM imidazole, and 1 mM β -ME]. The PriB variants were further purified with a S100 column equilibrated and washed with S100 Buffer [0.1 M NaHCO_3 (pH 9.0), (v/v) 20% glycerol, 500 mM NaCl, and 1 mM β -ME]. The PriB containing fractions were collected and I measured the concentration using UV-spectrophotometer at 280 nm.

The same 20-fold dye solution of FITC in DMSO was used. I incubated the protein solution with the dye solution avoiding light at room temperature for 1 hour. The reaction was stopped by incubating the mixture of protein and dye

with 0.1 ml 1 M Tris-HCl (pH 8.5) for 1 hour at room temperature. A second nickel column was employed to harvest the labeled PriB. Ni-NTA slurry was added to the yellow mixture and the mixture was incubated for 1 hour at room temperature. The mixture was transferred to a column and washed with 20 ml Wash Buffer [10 mM Tris-HCl (pH 8.5), (v/v) 20% glycerol, 100mM NaCl, and 1 mM β -ME] until the flow through was colorless and eluted by 10 ml Elution Buffer [10 mM Tris-HCl (pH 8.5), (v/v) 20% glycerol, 100 mM NaCl, 1 mM β -ME and 500 mM imidazole]. 100 units of thrombin was added to the elutant and the mixture was dialyzed in Dialysis Buffer[10 mM Tris-HCl (pH 8.5), (v/v) 20% glycerol, 100 mM NaCl, and 1 mM β -ME] overnight at 4°C.

I added 2 ml Ni-NTA slurry to the mixture solution and incubated them for 1 hour at 4°C and collected the flowthrough and concentrated it directly. The concentration was measured by the UV-Spectrophotometer with wavelengths 280 nm and 494 nm and calculated following the same instructions with the wild-type PriB. For K34A, A_{280} is 0.3306, A_{494} is 0.29856, A_{protein} is 0.2410, C_{protein} is 0.172 g/L and DOL is 29.19%; For K81A, A_{280} is 0.5021, A_{494} is 0.2619, A_{protein} is 0.4236, C_{protein} is 0.303 g/L and DOL is 14.56% For Y21A, A_{280} is 0.4187, A_{494} is 0.2896, A_{protein} is 0.3318, C_{protein} is 0.237 g/L and DOL is 20.57%; For E41A, A_{280} is 0.6526, A_{494} is 0.2462, A_{protein} is 0.5787, C_{protein} is 0.413 g/L and DOL is 10.02 %.The FITC-labeled PriB variants were stored at -80°C.

II-5 Fluorescence polarization spectroscopy

In the PriA-PriB-DnaT DNA replication restart pathway of *E. coli* cells, replication fork reactivation is mainly governed by weak individual interactions among primosome proteins PriA, PriB, and DnaT²⁹. The genome of *N. gonorrhoeae* encodes the homologs of PriB and PriA proteins but does not encode DnaT. So in my research, I examined protein:protein interactions between *N. gonorrhoeae* PriB and *N. gonorrhoeae* PriA and protein:nucleic acid interaction between *N. gonorrhoeae* PriB and ssDNA using fluorescence polarization spectroscopy experiments and affinity pull-down experiments.

Fluorescence polarization (FP) spectroscopy is a particularly robust and versatile technique to measure the protein:protein and protein: nucleic acid interactions, which has a long history in use. The theory of fluorescence polarization, first described in 1926 by Perrin³⁰, is based on the observation that fluorescent molecules in solution, excited with plane-polarized light, will emit light back into a fixed plane (i.e. the light remain polarized) if the molecules remain stationary during the excitation of the fluorophore. Molecules, however, rotate and tumble and the planes into which light is emitted can be very different from the plane used for initial excitation. It was first used as a tool for structural investigations of the binding of small molecules to protein in 1953³¹, and was described as a fluorescence polarization immunoassay in 1973.

In FP experiments, fluorescence anisotropy which assays the rotational diffusion of a molecule from the decorrelation of polarization in

fluorescence, i.e., between the exciting and emitted (fluorescent) photons, is usually used. This decorrelation can measure the "tumbling time" of the molecule as a whole, or of a part of the molecule relative to the whole. Now, there are two methods commonly used for measuring fluorescence anisotropy: L-format method and T-format method³². In the L-format method, a single emission channel is used, while the T-format method makes use of separate channels in which the parallel and perpendicular components are observed simultaneously³³. These two methods have different efficiencies for detecting various polarized components of fluorescent emission. Here I used the L-format method that is the most commonly used method.

In L-format or one channel method, excitation and emission wavelengths are selected with monochromators. The incident light is partially polarized by the excitation monochromator. An effect of this is that different intensities of the incident light will be generated depending on whether the excitation polarizer is in the horizontal or vertical position. In a similar manner, there will be different transmission efficiencies by the emission monochromator for vertically and horizontally polarized light (Figure 6)³³. The equation of fluorescence anisotropy (r) is^{32, 34-36}.

$$r = (I_{||} - I_{\perp}) / (I_{||} + 2 I_{\perp})$$

While that of polarization is:

$$p = (I_{||} - I_{\perp}) / (I_{||} + I_{\perp})$$

where, $I_{||}$ is the fluorescence intensity of vertically polarized emission and I_{\perp} is the intensity of horizontally polarized.

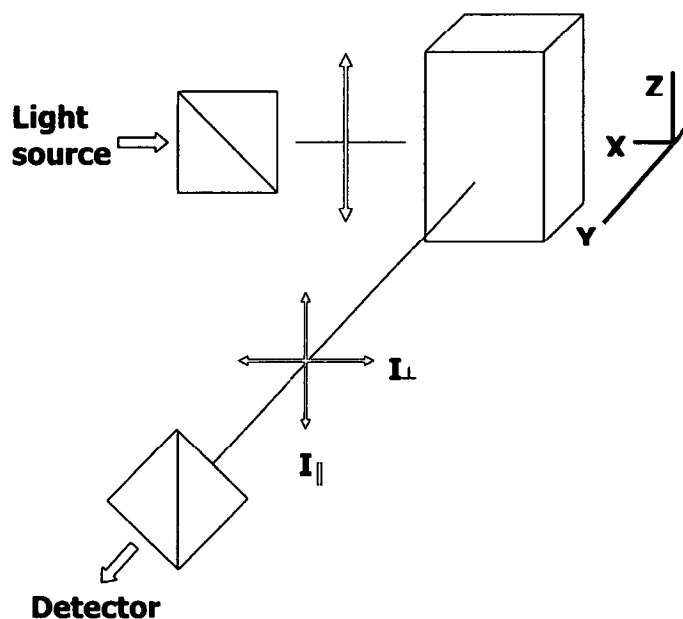


Figure 6. Schematic layout of the general L-format fluorescence polarization spectroscopy equipment ³³.

In solution, tumbling of fluorescently labeled molecules determines the polarization or anisotropy. Tumbling is a property that relies on factors such as temperature, viscosity, and most important molecular mass. If a molecule is small, rotation and tumbling is faster and the emitted light is depolarized relative to the excitation plane leading to a low anisotropy. If a molecule is very large, little movement occurs during excitation and the emitted light remains highly polarized producing a high anisotropy.

FP experiments need at least one fluorophore which is one of the interacting partners. A fluorophore is typically a very small molecule compared to the analyte. If there is an interaction between the fluorophore and the analyte, the fluorescence anisotropy difference between bound and unbound states is

obvious due to the heavier complex of the fluorophore and analyte (Figure 7). In this case, when I titrate the fluorophore with analyte, I can get an analyte-dependent increase in fluorescence anisotropy and draw a curve of anisotropy versus concentration of analyte. Furthermore, this curve can also allow kinetic studies of protein:protein and pretein:nucleic acids interactions as well as measurement of equilibrium binding constants.

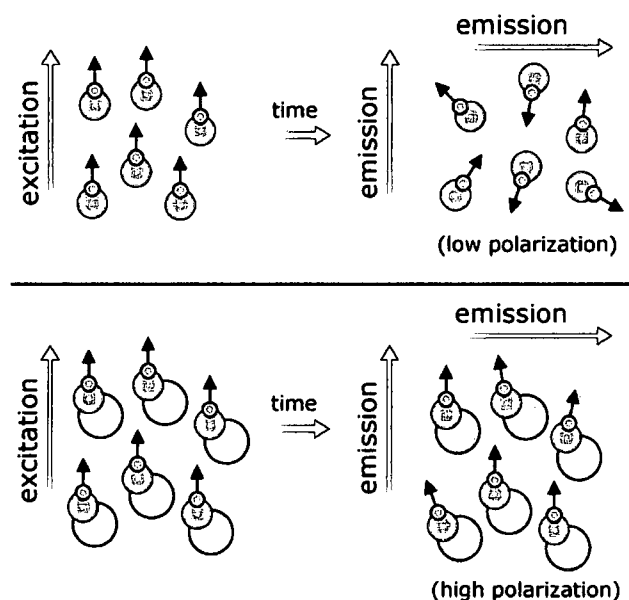


Figure 7. Fluorescence anisotropy facilitates detection of macromolecule interactions. Fluorescently labeling a smaller molecule (blue) with a fluorescent dye (green) produces the fluorophore. After it is excited, the emission is depolarized due to tumbling, which leads to a low fluorescence anisotropy. But if the small molecule can bind a big molecule (yellow), the emission is still polarized due to the heavier complex of them, producing a high fluorescence anisotropy.

In my FP experiments, I used FITC to label ssDNA and *N.gonorrhoeae* PriB variants, including wild-type *N.gonorrhoeae* PriB, E41A, Y21A, K34A, and

K81A, in order to elucidate the interactions between ssDNA and *N. gonorrhoeae* PriB and interactions between *N. gonorrhoeae* PriB and *N. gonorrhoeae* PriA, respectively. For the protein:nucleic acid interactions between *N. gonorrhoeae* PriB and ssDNA, a series of *N. gonorrhoeae* PriB solutions were made with a concentration range from 0 nM to 10,000 nM in FP buffer and incubated with a constant concentration of 10 nM FITC-ssDNA. All the mixtures were incubated for 15 min at room temperature before the first measurement and 3 sets of fluorescence anisotropies were measured every 15 min. For the protein:protein interactions between *N. gonorrhoeae* PriB and *N. gonorrhoeae* PriA, the PriA solutions were made in FP buffer using the same concentration range and incubated with a constant concentration of 10 nM FITC-PriB. All the data was collected following the same way with the protein:nucleic acids interactions. The fluorescence anisotropy was plot versus the concentration of the analytes. Because the fluorophore, including FITC-ssDNA and FITC-PriB, are small molecules, If there was no interaction, the fluorescence anisotropy in the plot was low even with a large molar excess of the analytes. If interaction exists, as I increased the concentration of PriB or PriA, the anisotropy should increase and saturate. The concentration when half of the binding sites are occupied is called the apparent K_D value. The lower the K_D is, the more robust the interaction is.

II-6 Affinity Pull-down experiments

The affinity pull-down experiment is also a powerful method used to determine physical interaction between two or more proteins. Affinity pull-down

experiments are useful for both confirming the existence of a protein:protein interaction predicted by other research techniques and as an initial screening assay for identifying previously unknown protein:protein interactions. The minimal requirement for an affinity pull-down experiment is the availability of a purified and tagged protein (the bait) which will be used to capture and pull down a protein-binding partner (the prey). The prey does not have the ability to bind with tag-specific affinity resin, which are often agarose-beads. And the buffer that is used in an affinity pull-down experiment contains some ingredient to block nonspecific interactions between agarose-beads and the prey. As a result, if only prey is mixed with agarose-beads, no prey can be pulled down. However, the prey can be pulled down in the presence of bait protein if it can interact with the bait protein. The result of affinity pull-down experiment can be checked with SDS-PAGE (Figure 8).

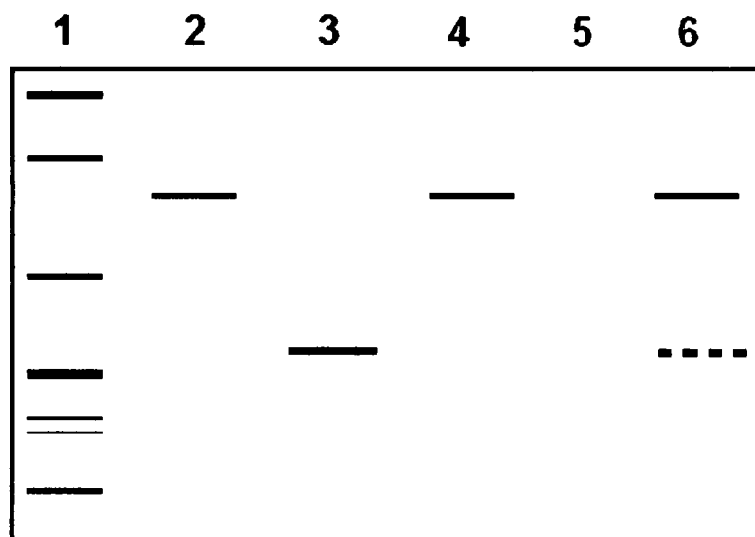


Figure8. Idealized gel electrophoresis analysis of protein:protein interactions using an affinity pull-down experiment. 1. protein marker; 2. purified bait input; 3. purified prey input, 4. purified bait pulldown, 5. purified

prey pulldown, and 6. bait: prey complex pulldown. Because prey protein can not bind agarose-beads, no protein will be pulled down in lane 5. However, if the prey can interact with the bait, it can be pulled down in lane 6 at the position of the dash line. If there is no interaction between the prey and bait protein, the band at this position will not appear.

In my research, affinity pull-down experiments were employed to detect a physical interaction between *N. gonorrhoeae* PriB and *N. gonorrhoeae* PriA. The bait is His-tagged *N. gonorrhoeae* PriA which can bind to the agarose-Ni beads (tag-specific affinity resin that I used). And the prey is *N. gonorrhoeae* PriB variants, including wild-type *N. gonorrhoeae* PriB, E41A, Y21A, and K34A mutants (Figure 9). If *N. gonorrhoeae* PriB variants can bind with *N. gonorrhoeae* PriA, I can detect *N. gonorrhoeae* PriB in SDS-PAGE. And in the buffer, BSA was used to block nonspecific interactions between proteins and Ni beads.

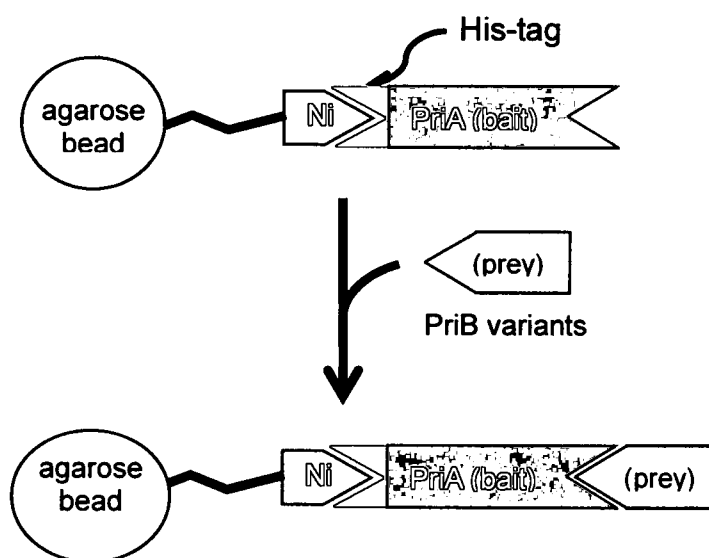


Figure 9. The workflow of an affinity pull-down experiment. *N.gonorrhoea*

PriA is the bait that can interact with Ni beads through its His-tags, and

N.gonorrhoeae PriB variants are the prey.

His-PriA and tagless PriB proteins were diluted to $1 \text{ g} \cdot \text{L}^{-1}$ in 10 mM Tris·HCl pH 8, 10% (v/v) glycerol, 0.1 M NaCl, 10 mM imidazole, 1 mM β -mercaptoethanol, $50 \text{ g} \cdot \text{L}^{-1}$ BSA and incubated either separately or together at a 1:3.5 molar ratio of His-PriA:PriB(dimers) for 30 min at 4°C . Nickel-NTA agarose beads were added to each sample, incubated for 10 min at 4°C , and collected by centrifugation at $21,130 \times g$ for 2 min at 4°C . The beads were washed several times in 10 mM Tris·HCl pH 8, 10% (v/v) glycerol, 0.1 M NaCl, 10 mM imidazole, 1 mM β -mercaptoethanol, $50 \text{ g} \cdot \text{L}^{-1}$ BSA, and collected after each wash by centrifugation at $21,130 \times g$ for 2 min at 4°C . Pulldown products were eluted by addition of SDS-PAGE sample buffer. The products were resolved through a 13.5% polyacrylamide gel and visualized by coomassie brilliant blue staining.

II-7 Crystallization of PriB:single-stranded DNA complexes

Knowledge of the three-dimensional structure of a macromolecule is of great importance in understanding its function. The structural research here employed X-ray crystallography to study structure/function relationships of proteins involved in rescuing DNA replication complexes following DNA damage.

Crystallography is a scientific study of crystals and crystal formation through determining the arrangement of atoms in crystals. X-ray crystallography is a crystallographic method which uses X-ray as the radiation source to interact with valence electrons. It has been the most commonly used method, especially in biological study of macromolecules. This method can reveal the structure and functioning of many biological molecules, including vitamins, drugs, proteins and nucleic acids based on the X-ray diffractions of their crystals. Since the first success of using X-ray crystallography to solve protein structure in late 1950s³⁷, over 48,970 X-ray crystal structures of proteins, nucleic acids and other biological molecules have been determined³⁸.

The reason why X-ray crystallography is so useful in detecting the structure of macromolecule can be explained using physical theories. In physics, we know that in order for the object to diffract light and thus be visible under magnification, the wavelength of the light should be no larger than the object. In macromolecules, the bonded atoms are about 1.5 angstroms apart which falls into X-ray (0.1-10 angstroms) range. But X-ray crystallography can not be used to detect the structure of a single molecule. There are two reasons. The first reason is that X-ray can not be focused by glass lenses and the second one is that a single molecule is a very weak scatter of X-ray. So using X-ray crystallography, we only can get an X-ray diffraction pattern of a crystal (Figure 10). Because in crystals, the diffracted beams for all molecules augment each other to produce a strong, detectable X-ray diffraction pattern. And the macromolecule structure then can be solved by mathematical analysis of the X-ray diffraction pattern.

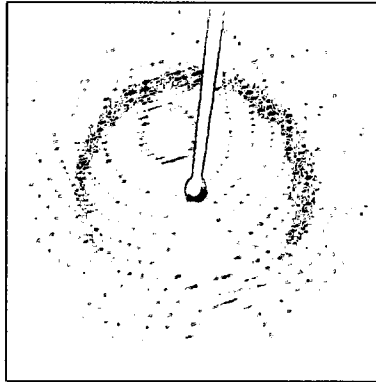


Figure 10. X-ray diffraction pattern of a protein crystal. Each dot in this figure, called a reflection, forms from the coherent interference of scattered X-rays passing through the crystals³⁹.

Generally speaking, four steps are involved in X-ray crystallography experiment. The first and often most difficult step is to grow crystals. The crystal should be sufficiently large, pure in composition and regular in structure, with no significant internal imperfections such as cracks or twinning. After we get good enough crystals, we can place the crystals in an intense X-ray beam, usually monochromatic X-rays, to get regular pattern of reflection. As the crystal is gradually rotated, previous reflections disappear and new ones appear, the intensity of every spot is recorded at every orientation of the crystal. Multiple data sets may have to be collected, with each set covering slightly more than half a full rotation of the crystal and typically containing tens of thousands of reflection intensities. In the third step, these data are combined computationally to map the electron density of the structure. Last but not least is using the electron density map with complementary chemical information to

produce and refine a model of the arrangement of atoms within the crystal (Figure 11).

In my research, the protein crystals were developed using hanging-drop vapor diffusion method. The hanging-drop vapor diffusion technique is the most popular method for the crystallization of macromolecules. The principle of this method is shown as follows (Figure 12). A drop composed of sample and reagent is placed in vapor equilibration with a liquid reservoir solution. Typically the drop contains a lower reagent concentration than the solution. To achieve equilibrium state, water leaves the drop by vapor diffusion and eventually ends up in the solution. Loss of water from the drop by vapor diffusion increases the concentration of protein in the drop, leading to supersaturation and crystal growth. For different proteins, the reservoir solutions are different. But the solutes should be always hygroscopic, which are intent to withdraw water from the drop on lid. I used PEG 4000 (polyethylene glycol), PEG 8000, MES buffers with different pHs (2-(N-morpholino) ethanesulfonic acid), NaCl, and glycerol in the reservoir solution to screen for crystals.

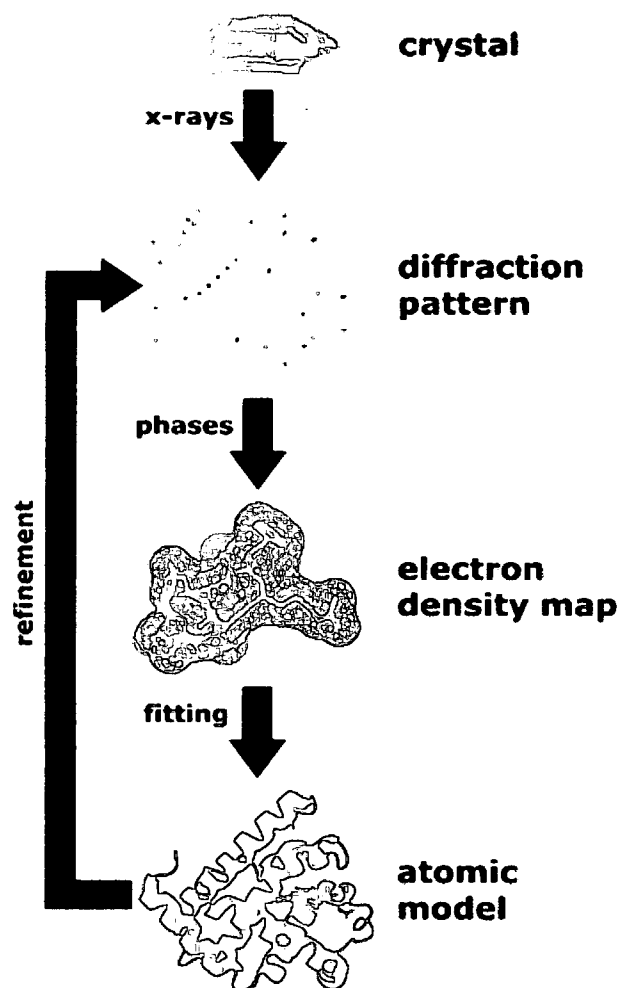


Figure 11. Workflow for solving the structure of a molecule by X-ray crystallography⁴⁰.

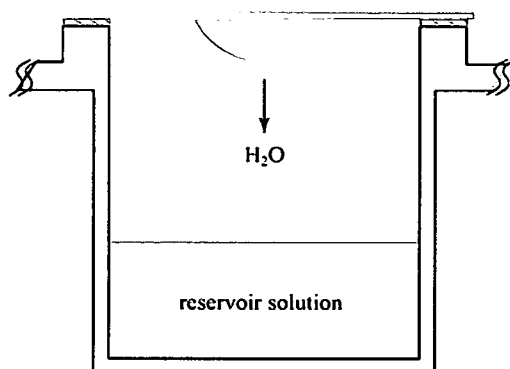


Figure 12. Diagram of hanging-drop vapor diffusion method. The lid was adhered to the well with vacuum grease to prevent water vapor loss to the air which would dry the drop⁴¹.

The structures of crystals with good morphology got using this method were solved using X-ray diffraction data collected at the Advanced Photon Source at the Argonne National Laboratories. Crystallographic phasing was performed using molecular replacement with the crystal structure of *E. coli* PriB as a search model (PDB code 1V1Q).

CHAPTER III

RESULTS AND DISCUSSION

III-1 *N.gonorrhoeae* PriB is a single-stranded DNA-binding protein

Our laboratory has recently solved a crystal structure of *N. gonorrhoeae* PriB at 2.7 angstroms resolution. *N. gonorrhoeae* PriB is a homodimer comprised of a single structural domain consisting of two oligosaccharide/oligonucleotide binding (OB) folds that has a high degree of structural similarity to that of *E. coli* PriB (Figure 13). In each of its OB folds, there are five secondary structure β strands that are antiparallel with each other and connected by loops to form a β barrel structure. All the structural components are spatially arranged in a way that is similar to *E. coli* PriB. The β strands in this structure almost overlap with the β strands in the structure of *E. coli* PriB. The structural similarity between these two homologs of PriB support the hypothesis that *N. gonorrhoeae* PriB is a ssDNA-binding protein and suggest that *N. gonorrhoeae* PriB binds ssDNA via the classical ligand binding surface of its OB folds.

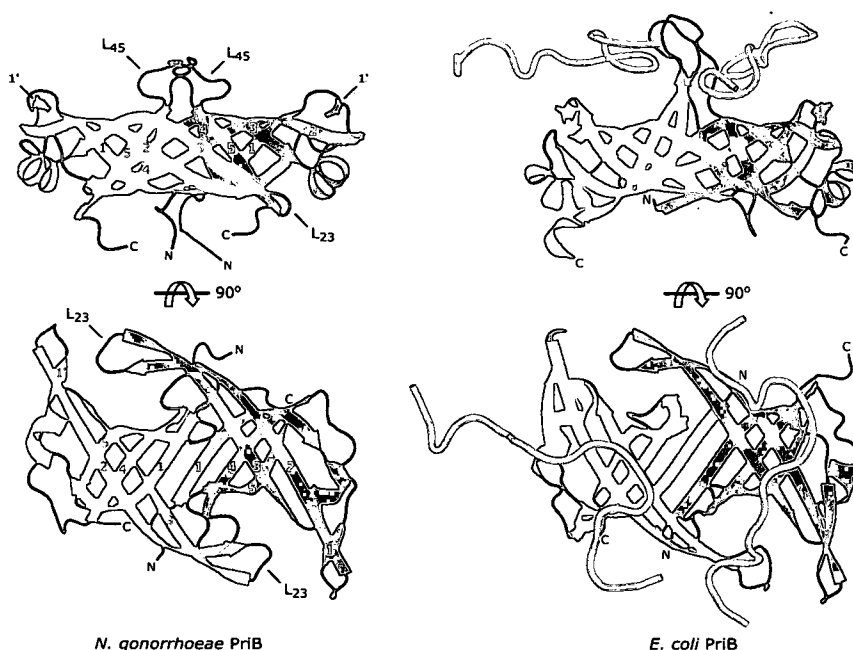


Figure 13. Orthogonal views of the crystal structures of *N. gonorrhoeae* PriB and *E. coli* PriB²⁹. Each PriB homolog has two OB folds that are shown in blue and red. The cyan loops on the structure of *E. coli* PriB represent the ssDNAs binding to *E. coli* PriB on its classic ligand binding surface.

To test the hypothesis that *N.gonorrhoeae* PriB binds ssDNA via the classic ligand binding surface of its OB folds, I attempted to crystallize PriB in the presence of ssDNA . I used the hanging-drop vapor diffusion method and was able to grow crystals whose morphology is distinct from that of PriB crystals grown in the absence of ssDNA (Figure 14). The morphology of these crystals grown in the presence of ssDNA is hexagonal which is different from the tetragonal apo-PriB crystals.

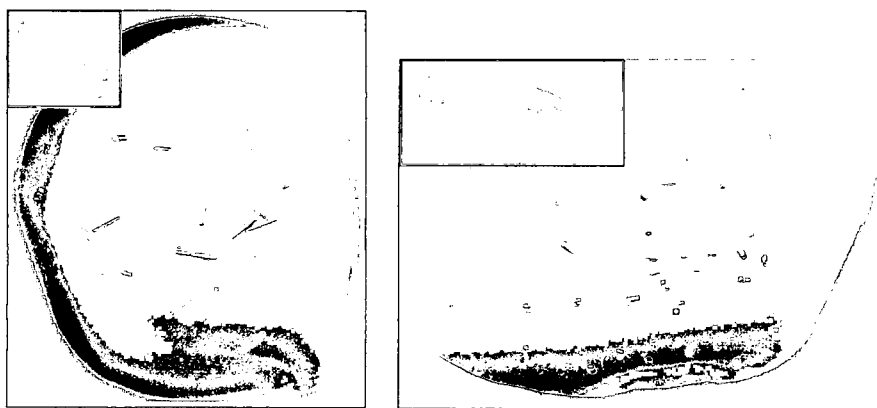


Figure 14. Crystals of *N. gonorrhoeae* PriB grown in the absence (left) and presence (right) of ssDNA.

Although these crystals diffract X-rays to approximately 3 angstroms resolution, we were not able to resolve any electron density in the crystals that could be attributed to ssDNA. It appears that the ssDNA is either not present in the crystals or is not well-ordered in the crystals.

Our laboratory performed equilibrium DNA binding experiments using fluorescence polarization spectroscopy and determined that PriB binds ssDNA *in vitro* and shows a slight preference for oligonucleotides of approximately 36 bases in length. Therefore, I chose a 36-base oligonucleotide to study the binding sites for ssDNA on *N. gonorrhoeae* PriB in my FP experiments.

III-2 Identification of PriB's Binding site for ssDNA

In order to map the binding sites of ssDNA on *N. gonorrhoeae* PriB, I used site-directed mutagenesis to introduce single alanine substitutions into *N.*

gonorrhoeae PriB. Since the binding sites for ssDNA on *E. coli* PriB are on the classic ligand binding surface, I chose three residues on the analogous surface of *N. gonorrhoeae* PriB to substitute with alanine: K81, K34 and Y21 (Figure 15). I also substituted E41 with alanine since this residue has been shown to be important for the interactions with PriA in *E. coli*.

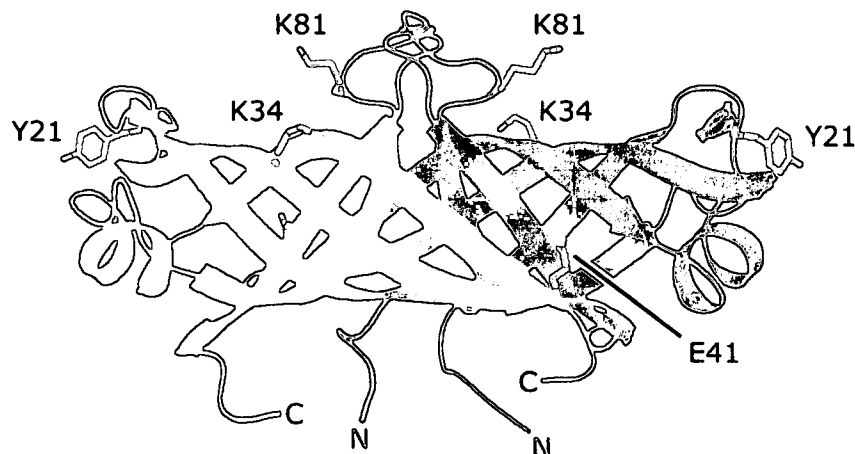


Figure 15. Locations of substituted amino acid residues. The top surface in this rendering is the classic ligand-binding surface for related OB-fold proteins. Since *N. gonorrhoeae* PriB is a homodimer, each variant contains two symmetrical amino acid substitutions that were introduced through site-directed mutagenesis.

I employed equilibrium binding studies in which the fluorescence anisotropy of FITC-ssDNA was measured in the presence and absence of each PriB variants (Figure 16).

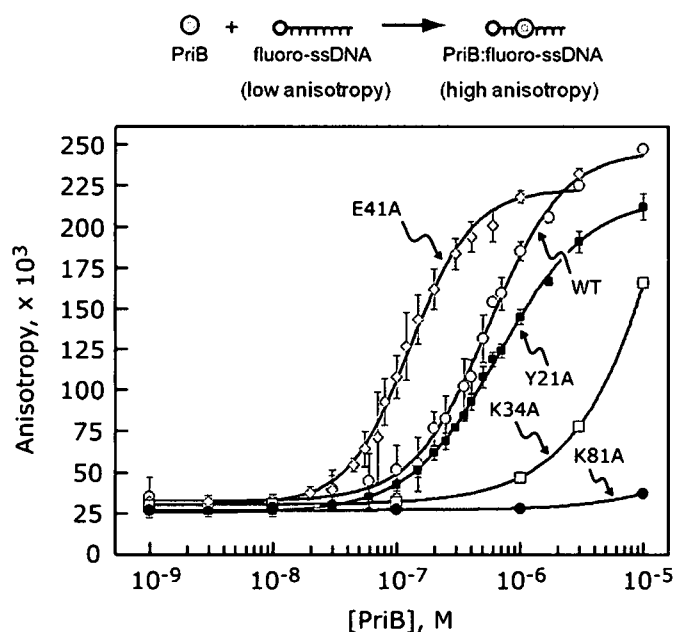


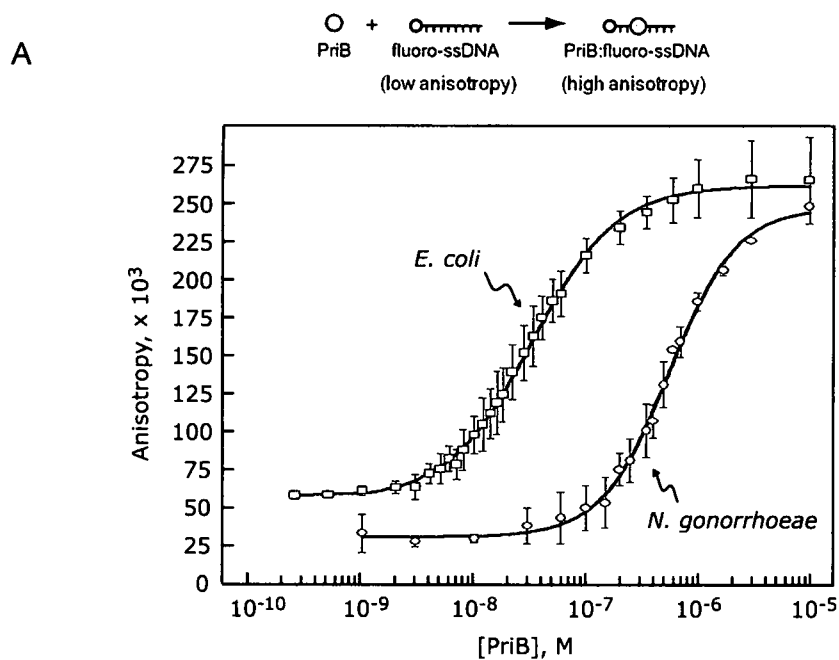
Figure 16. *N. gonorrhoeae* PriB variants have altered ssDNA binding activities. Compared to PriB variants, FITC-ssDNA is small and has a low fluorescence anisotropy, which can be increased due to the formation of a complex. In these plots, a shift in a curve towards the right means a weaker interaction between the fluorophore and the analyte. A shift in the curve towards the left means a stronger interaction. This plot reveals that the interactions between K81A and K34A variants and ssDNA are weaker than that of wild-type PriB.

As expected, I found out important information for the interaction between PriB and ssDNA. The Y21A variant shows only a modest defect in ssDNA binding with a K_D of 641.6 nM, compared to a K_D of 474.7 nM for wild-type PriB. However, other variants K81A and K34A show significant defects in ssDNA binding. The interaction with ssDNA is so weak for these variants that an apparent K_D values can not be determined in this way. The anisotropy did not

increase even with a 1,000-fold molar excess of K81A and K34A to FITC-ssDNA. These results suggest that these two residues are important for the interaction between *N.gonorrhoeae* PriB and ssDNA. Both of these K34 and K81 residues are on the surface of PriB near to the L₄₅ loops, so I can conclude that the ssDNA binding site on PriB lies along the L₄₅ loops and adjacent β strands and involves contributions from basic residues such as K34 and K81. And for E41A variant that is located in the shallow pocket near to the L₂₃ loop (Figure 15) enhances the interaction between the ssDNA and PriB. This enhancement is likely due to the reducing of charge repulsion forces between ssDNA and the side chains of the acidic residues. Although E41 lie at the dimerization interface, mutation to alanine does not likely result in a misfolded PriB. The evidence is that the E41A variant has a same retention volume with wild-type *N. gonorrhoeae* PriB in the same size-exclusion column, suggesting that they have similar structures.

Interestingly, the K_D of wild-type *N. gonorrhoeae* PriB for ssDNA indicates that the interaction between *N. gonorrhoeae* PriB and ssDNA is approximately 16-fold weaker than that between *E. coli* PriB and ssDNA (Figure 17A)²⁵. The difference could be explained by the different charge distribution on the surface of the *N. gonorrhoeae* PriB and *E.coli* PriB (Figure 17B). On the surface of the structure, especially on the L₄₅ loops side, *E. coli* PriB has much more positive charge density than *N. gonorrhoeae* PriB does. The less positive charges there are, the weaker the interaction between ssDNA and PriB is. This is also consistent with my hypothesis that *N. gonorrhoeae* PriB binds with ssDNA via the classic ligand binding surface of its OB fold. But the difference in

the binding affinity shows that differences exist between *E. coli* DNA replication restart mechanisms and the mechanism of DNA replication restart in *N. gonorrhoeae*. In *E. coli* cells, another primosome protein called DnaT exists and it competes with ssDNA for binding to *E. coli* PriB²⁹, which is supported by observations that addition of *E. coli* DnaT to *E. coli* PriB: FITC-ssDNA results in a decrease in fluorescence anisotropy as FITC-ssDNA is released from *E. coli* priB. But in *N. gonorrhoeae* cells, no homolog of DnaT is encoded, suggesting that *N. gonorrhoeae* cells might use a distinct mechanism to recruit the replisome to a repaired DNA replication fork.



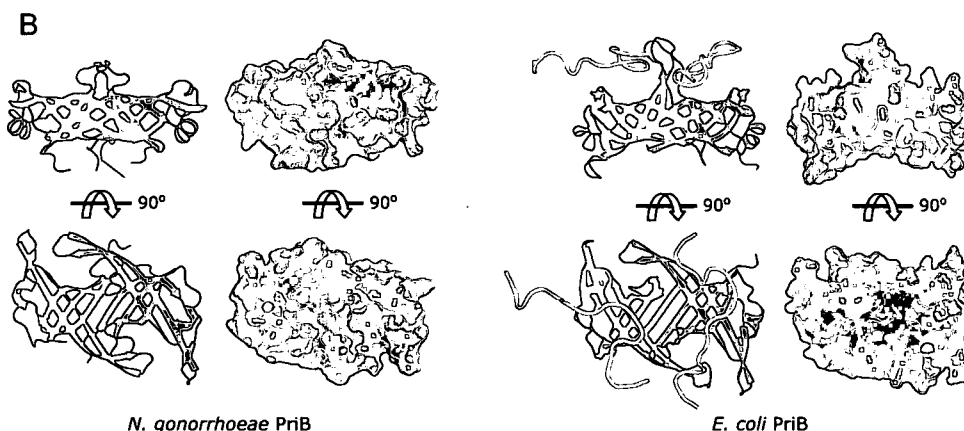


Figure 17. *N.gonorrhoeae* PriB and *E.coli* PriB differ in their ssDNA binding activity and surface charge properties. A). *N. gonorrhoeae* PriB binds ssDNA weaker than does *E. coli* PriB²⁵. Both of them can bind FITC-ssDNA to produce analyte-dependent increase in anisotropy, but it needs more *N. gonorrhoeae* PriB to saturate. B). The solvent-accessible surface charge potential distribution of the *N. gonorrhoeae* PriB and *E.coli* PriB homologs are different. The positive charge potential on the surface of PriB can be used to interact with ssDNA. *E. coli* PriB has more positive charge density, especially on its binding surface, so that it has a higher binding affinity than *N. gonorrhoeae* PriB. the surface view are colored according to electrostatic surface potential at +/- 10 Kt/e for positive(blue), negative (red), or zero (white) charge potential.

III-3 *N. gonorrhoeae* PriB physically interacts with *N.gonorrhoeae* PriA

In addition to protein:nucleic acid interactions, numerous protein:protein interactions lie at the heart of DNA replication restart primosome function. I employed FP experiments to detect whether direct physical interactions exist

between PriB and PriA by measuring the fluorescence anisotropy of FITC-labeled *N.gonorrhoeae* PriB in the presence and absence of *N.gonorrhoeae* PriA. In *E. coli* cells, PriB only interacts with PriA in the presence of DNA²⁹. The DNA binding induces a conformational change in *E. coli* PriA that exposes the PriB binding site to bind with *E. coli* PriB²⁹. Based on this observation, I predicted that there is no direct interaction between *N. gonorrhoeae* PriA and *N. gonorrhoeae* PriB which means I can not get a PriA-dependent increase in fluorescence anisotropy in my FP experiments when I titrate FITC-PriB solution only with PriA.

Contrary to my prediction, as I increased the concentration of PriA, I observed a PriA-dependent increase with a K_D value of 140 nM which saturates at the PriA's concentration of 1,000 nM in the fluorescence anisotropy (Figure 18). This indicates that *N.gonorrhoeae* PriB has direct and robust physical interaction with *N. gonorrhoeae* PriA while *E. coli* PriB only interacts with *E. coli* PriA in the presence of DNA²⁹. What's more, the interaction is species specific. When I repeated the same FP experiment using *N.gonorrhoeae* PriB and *E. coli* PriA, only a modest increase was observed even in the presence of 1,000-fold molar excess of *E. coli* PriA relative to FITC- *N.gonorrhoeae* PriB, indicating a weak interaction. This evidence verifies the specificity of the interaction between *N.gonorrhoeae* PriB and *N.gonorrhoeae* PriA.

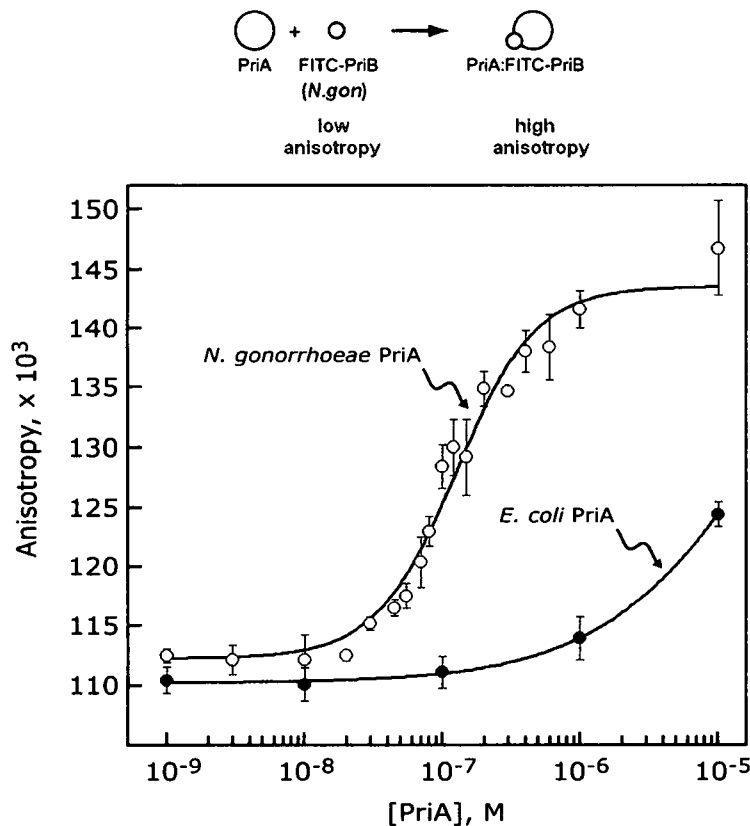


Figure 18. *N. gonorrhoeae* PriA and PriB form a complex that is species specific. The low fluorescence anisotropy of FITC-PriB (approximately 11.45 KD) can be increased if it binds PriA (81.13 KD). When FITC-PriB is titrated with *N. gonorrhoeae* PriA, its anisotropy increases and saturates at approximately 10⁻⁶ M *N. gonorrhoeae* PriA, suggesting a direct, physical interaction exists between them. However, the curve is significantly right-shifted and no saturation appears even with a high concentrations of *E. coli* PriA, indicating there is no interaction is between *N. gonorrhoeae* PriB and *E. coli* PriA.

III-4-1 Identification of PriB's binding sites for PriA using affinity pull-down experiments

To test the hypothesis that the binding sites for *N. gonorrhoeae* PriA overlap with those for ssDNA on *N. gonorrhoeae* PriB, I employed affinity pull-down experiments to test the interactions between *N. gonorrhoeae* PriB and *N. gonorrhoeae* PriA. Affinity pull-down experiments are a powerful technique to detect protein:protein interactions. It is useful for both confirming the existence of a protein:protein interaction predicted by other research techniques and as an initial screening assay for identifying previously unknown protein:protein interactions. The minimal requirement for an affinity pull-down experiment is the availability of a purified and tagged protein (the bait) which will be used to capture and pull down a protein-binding partner (the prey).

At first, I tested the ability of *N. gonorrhoeae* PriA and wild-type *N. gonorrhoeae* PriB to interact under conditions of varying ionic strength. For these experiments, I tested NaCl at 50 mM, 100 mM, 150 mM, 200 mM, 250 mM, 300 mM, 400 mM and 500 mM. I found that in 100 mM NaCl solution, the band on the SDS-PAGE for PriB was the strongest, suggesting that the interaction between *N. gonorrhoeae* PriB and *N. gonorrhoeae* PriA was the most robust under this condition. Based on these results, Buffer A [10 mM Tris-HCl (pH 8.0), (v/v) 10% glycerol, 100 mM NaCl, 10 mM imidazole and 1 mM β -ME] was used to make 1 g/L solutions of *N. gonorrhoeae* PriA and *N. gonorrhoeae* PriB variants and Buffer B [10 mM Tris-HCl (pH 8.0), (v/v) 10% glycerol, 100 mM NaCl, 10 mM imidazole, 1 mM β -ME and 50 g/L BSA] was used to dilute Ni-NTA beads. I also tried three different molar ratios: 1:1, 1:2

and 1:7 of PriA:PriB and the results show the greatest amount of association between PriA and PriB when the proteins are mixed at a ratio of 1:7.

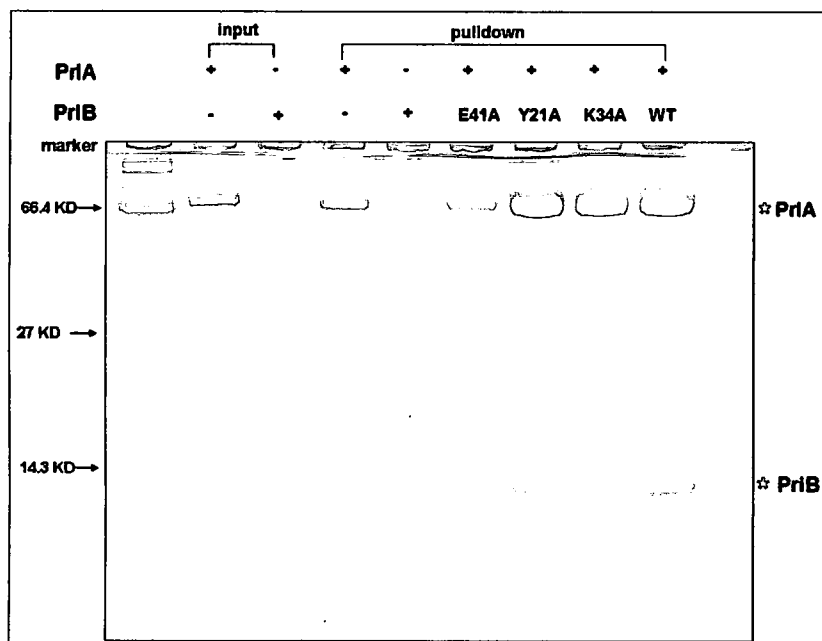


Figure 19. Affinity pull-down experiments with *N.gonorrhoeae* PriA and PriB. Some of the *N. gonorrhoeae* PriB variants were pulled down by *N. gonorrhoeae* PriA, while some were not. Wild-type *N. gonorrhoeae* PriB input can be shown on the gel. However, no PriB was on the gel in the second pull-down trial with PriB itself. The bands for PriB appeared on the gel only when PriA was added.

After I got the right buffer and molar ratio, I tested wild-type *N. gonorrhoeae* PriB, E41A, Y21A and K34A (I did not get enough K81A due to its low solubility) (Figure 19). The results indicated that wild-type *N. gonorrhoeae* PriB was pulled down by *N. gonorrhoeae* PriA, indicating the interaction between them

exists. And for the PriB variants, Y21A has a band that is similar to the wild-type PriB; K34A showed some defect in the binding ability; while no E41A was pulled down.

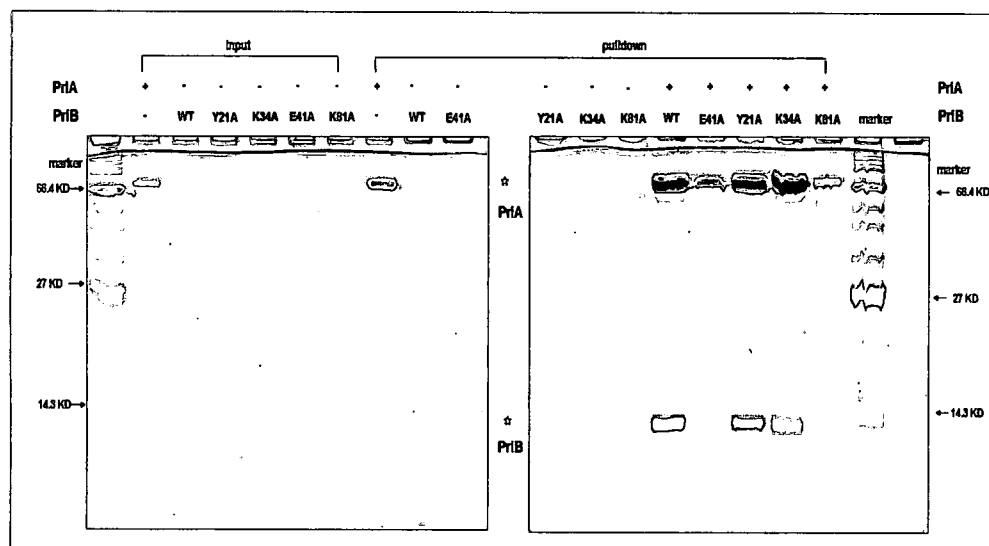


Figure 20. *N. gonorrhoeae* PriB variants were pulled down by PriA except E41A and K81A. The different intensities of the input on the gel might be caused by the mutagenesis. The Ni beads did not pull down any PriB variants in the absence of PriA. Even in the presence of PriA, E41A and K81A were not pulled down, suggesting defects in their binding ability to PriA introduced by alanine substitution. The binding ability of another variant K34A was also weakened.

In conclusion, residues K34, E41, and K81 might be involved in the interaction between PriA and PriB. However, there were some obstacles to these affinity pull-down experiments that limit our ability to interpret them. The first one is that K81A had very low solubility in buffers so that I can not get enough sample to analyze using SDS-PAGE. The second one is that when I tried to input PriB

variants to the gel, I can not get a series of bands with the same intensity, even though I loaded equivalent amounts of them, which means that I can not get the information of how much PriB variants were pulled down compared to the inputs (Figure 20). Therefore, I went back to an FP-based approach to map the interaction between PriA and PriB.

III-4-2 Identification of PriB's Binding sites for PriA using FP experiments

For this part of FP experiments, I FITC labeled all the *N. gonorrhoeae* PriB variants to identify residues that are important for the PriB:PriA interaction (Figure 15). The fluorescence anisotropy of FITC-PriB variants in the presence and absence of *N. gonorrhoeae* PriA was measured. All the FP experiments were carried out under the same conditions as with wild-type PriB except that I used 30 nM of FITC-PriB variants.

Two PriB variants, E41A and K34A, showed significant defects in binding PriA, PriB variant Y21A did not show significant defect in PriA binding ability which has a K_D of 198.4 nM. And I did not analyze K81A variant because of its very low solubility. The result of E41A can be explained by its unique chemical environment of *N. gonorrhoeae* PriB (Figure 21). The residues around E41 on most of the known PriB homologs are conserved. However, *N. gonorrhoeae* PriB has a series of residues surrounding residue E41 which I think can explain the strong PriA binding ability of *N. gonorrhoeae* PriB. These residues, distinct from those on other PriB homologs, form a chemical environment that could make the interaction between PriA and PriB more favorable. The result

of K34A variant is interesting. In *E. coli* PriB structure, there is no analogous K34 residue. The analogous residue at this position is residue E42 which is not involved in the interaction between PriA and PriB. The unique chemical environment of residue E41 and different residue at the position where residue K34 lies could explain the high binding ability between *N. gonorrhoeae* PriA and PriB.

Following identification of PriB surface residues important for the PriA:PriB interaction and the PriB:ssDNA interaction, it became clear that overlap exists among PriB binding sites for PriA and ssDNA, akin to *E. coli* PriB. This overlap suggests that PriA and ssDNA might compete with each other for binding with PriB.

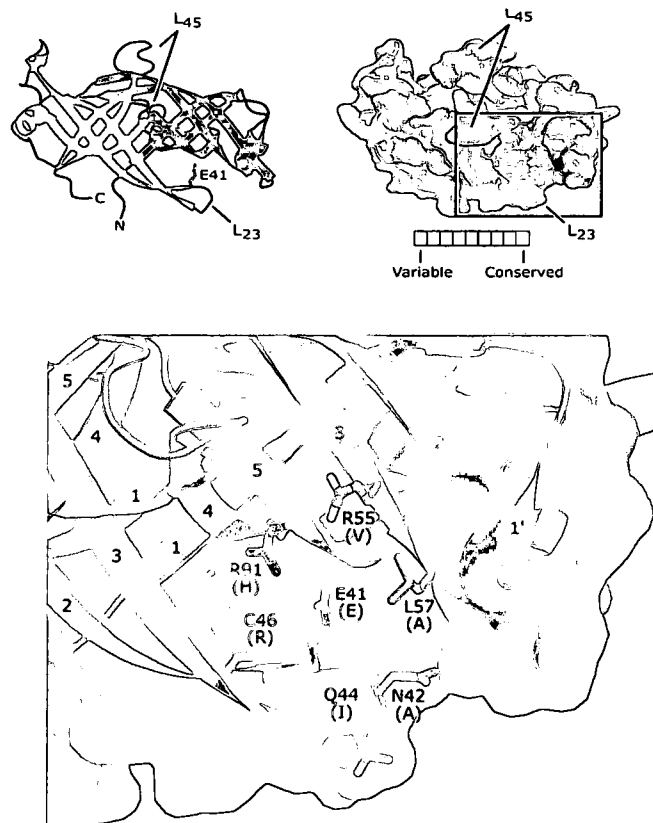


Figure 21. Variation of surface residues of PriB homologs. For all the sequenced PriB homologs, the residues around E41 residue are conserved. But in *N. gonorrhoeae* PriB, E41 residue has a unique chemical environment. This E41 residue is positionally conserved with the E39 residue of *E. coli* PriB and we hypothesize that this residue likely plays a role in interactions with PriA. At the position analogous to that of residue R44 of *E. coli* PriB lies residue C46 in the *N. gonorrhoeae* PriB homolog. This cysteine residue is unlikely to be involved in interactions with ssDNA and would not be able to participate in ionic interactions with E41. However, there are two arginine residues positioned near residue C46 in *N. gonorrhoeae* PriB, R55 and R91, that might serve the same role as R44 of *E. coli* PriB. Thus, the architecture of this shallow pocket has been remodeled in the time since *N. gonorrhoeae* and *E. coli* shared a common ancestor, although perhaps in a way that conserved its overall function as a binding site for PriA.

CHAPTER IV

CONCLUSIONS AND FUTURE DIRECTION

IV-1 Conclusions

In my experiments, because K81A variant had a very low solubility in the buffers that I used when I tried to purify it and it did not show any binding ability with ssDNA or *N.gonorrhoeae* PriA, I believe that the K81A variant does not fold correctly. As a result, I made all my conclusions based on the results of the other four variants: wild-type PriB, Y21A, E41A and K34A.

Based on the results of the structural and mechanistic study, I have been able to develop a model for the structure and function of *N. gonorrhoeae* PriB in DNA replication restart pathways. *N. gonorrhoeae* PriB is a homodimer that is comprised of a single structural domain consisting of two oligosaccharide/oligonucleotide binding (OB) folds, which is very similar to the structure of *E. coli* PriB.

N.gonorrhoeae PriB is a ssDNA-binding protein that binds ssDNA via the classic ligand binding surface of its OB folds, akin to *E. coli* PriB. An amino acid residue on this surface, K34, plays an important role in this interaction. However, this interaction has a lower affinity than that of *E. coli* PriB due to

less positive surface charges distributed on *N. gonorrhoeae* PriB's OB folds. In addition to the interaction between *N.gonorrhoeae* PriB and ssDNA, *N. gonorrhoeae* PriB has direct and robust physical interaction with *N. gonorrhoeae* PriA which is species specific. This interaction is significantly different from *E. coli* PriB that only can bind with *E. coli* PriA in the presence of DNA. From my experiments, I identified two amino residues that are important for this interaction: E41 and K34. What's more, the binding sites on *N. gonorrhoeae* PriB for *N.gonorrhoeae* PriA have overlap with the binding sites for ssDNA.

IV-2 Future Direction

The strength of interactions between PriB and ssDNA, and between PriA and PriB has not been well-conserved between *Neisseria gonorrhoeae* and *E. coli*. In the future, we are interested in obtaining high resolution models of *N. gonorrhoeae* PriB bound to ssDNA or to *N.gonorrhoeae* PriA to better understand their binding mechanisms. Through comparison between *N. gonorrhoeae* and *E. coli*, we can see some differences in the binding affinities between PriA and PriB, and PriB and ssDNA, so we would like to understand what the biological significance of these differences are. And we hope ultimately we can identify compounds that can disturb interactions between DNA replication restart proteins and develop these inhibitors as antibacterial agents that target *N. gonorrhoeae*.

REFERENCES

1. David L. Nelson and Michael M. Cox, Principles of Biochemistry. 2005. p.948-951.
2. Baker, T.A. and S.P. Bell, Polymerases and the replisome: machines within machines. Cell, 1998. 92(3): p. 295-305.
3. Cox, M.M., Recombinational DNA repair of damaged replication forks in *Escherichia coli*: questions. Annu Rev Genet, 2001. 35: p. 53-82.
4. Cox, M.M., et al., The importance of repairing stalled replication forks. Nature, 2000. 404(6733): p. 37-41.
5. McCool, J.d., C.C. Ford, and S.J. Sandler, A *dnaT* mutant with phenotypes similar to those of a *priA::kan* mutant in *Escherichia coli* K-12. Genetics, 2004. 167(2): p. 569-78.
6. Sandler, S.J., et al, *dna C* mutations suppress defects in DNA replication-and recombination-associated functions in *priB* and *priC* double mutants in *Escherichia coli* K-12. Mol Microbio., 1999. 34(1):p. 91-101.
7. Heller, R.C. and K.J. Mariani, The Disposition of Nascent Strands at Stalled Replication Forks Dictates the Pathway of Replication Restart during Resart. Mol cell, 2005. 17(5): p. 733-43.
8. Shafer, W. M., and R. F. Rest, Interactions of gonococci with

- phagocytic cells. *Annu. Rev. Microbiol.*, 1989. 43:p. 121–145.
9. Zheng, H. Y., T. M. Alcorn, and M. S. Cohen, Effects of H₂O₂-producing lactobacilli on *Neisseria gonorrhoeae* growth and catalase activity. *J. Infect. Dis.*, 1994. 170:p. 1209–1215.
 10. Parsons, N. J., A. A. Kwaasi, J. A. Turner, D. R. Veale, V. Y. Perera, C. W. Penn, and H. Smith, Investigation of the determinants of the survival of *Neisseria gonorrhoeae* within human polymorphonuclear phagocytes. *J. Gen. Microbiol.*, 1981. 127: p.103–112.
 11. Storz, G., and J. A. Imlay, Oxidative stress. *Curr. Opin. Microbiol.*, 1999. 2: p.188–194.
 12. Soler-Garcia, A. A., and A. E. Jerse, A *Neisseria gonorrhoeae* catalase mutant is more sensitive to hydrogen peroxide and paraquat, an inducer of toxic oxygen radicals. *Microb. Pathog.*, 2004. 37: p. 55–63.
 13. Seib, K. L., M. P. Jennings, and A. G. McEwan, A Sco homologue plays a role in defense against oxidative stress in pathogenic *Neisseria*. *FEBS Lett.*, 2003. 546: p. 411–415.
 14. Seib, K. L., H. J. Tseng, A. G. McEwan, M. A. Apicella, and M. P. Jennings, Defenses against oxidative stress in *Neisseria gonorrhoeae* and *Neisseria meningitidis*: distinctive systems for different lifestyles. *J. Infect. Dis.*, 2004. 190: p. 136–147.
 15. Turner, S., E. Reid, H. Smith, and J. Cole, A novel cytochrome c peroxidase from *Neisseria gonorrhoeae*: a lipoprotein from a gram-negative bacterium. *Biochem. J.*, 2003. 373: p. 865–873.
 16. Skaar, E. P., D. M. Tobiason, J. Quick, R. C. Judd, H. Weissbach, F. Etienne, N. Brot, and H. S. Seifert, The outer membrane localization of the

- Neisseria gonorrhoeae* MsrA/B is involved in survival against reactive oxygen species. *Proc. Natl. Acad. Sci.*, 2003. USA 99: p. 10108–10113.
17. Tseng, H. J., Y. Srikhanta, A. G. McEwan, and M. P. Jennings, Accumulation of manganese in *Neisseria gonorrhoeae* correlates with resistance to oxidative killing by superoxide anion and is independent of superoxide dismutase activity. *Mol. Microbiol.*, 2001. 40: p. 1175–1186.
 18. Kline, K. A., E. V. Sechman, E. P. Skaar, and H. S. Seifert, Recombination, repair and replication in the pathogenic *Neisseriae*: the 3 R's of molecular genetics of two human-specific bacterial pathogens. *Mol. Microbiol.*, 2003. 50: p. 3–13.
 19. Marians, K. J, PriA-directed replication fork restart in *Escherichia coli*. *Trends Biochem. Sci.*, 2000. 25: p. 185–189.
 20. McGlynn, P., A. A. Al-Deib, J. Liu, K. J. Marians, and R. G. Lloyd, The DNA replication protein PriA and the recombination protein RecG bind D-loops. *J. Mol. Biol.*, 1997. 270: p. 212–221.
 21. Nurse, P., J. Liu, and K. J. Marians, Two modes of PriA binding to DNA. *J. Biol. Chem.*, 1999. 274: p. 25026–25032.
 22. Sandler, S. J, Multiple genetic pathways for restarting DNA replication forks in *Escherichia coli* K-12. *Genetics*, 2000. 155: p. 487–497.
 23. Kimberly A. Kline and H. Steven Seifert, Mutation of the priA Gene of *Neisseria gonorrhoeae* Affects DNA Transformation and DNA Repair. *J. Bacteriology*, 2005. 187(15): p. 5347–5355.
 24. Liu, J.H., Chang, T.W., Huang, C.Y., Chen, S.U., Wu, H.N., Chang, M.C., and Hsiao, C.D., Crystal structure of PriB- a primosomeal DNA replication protein of *Escherichia coli*. *J. Bio. Chem.*, 2004. 279: p. 50465–50471.

25. Lopper, M., Holton, J.M., and Keck, J. L., Crystal structure of PriB. a component of the Escherichia coli replication restart primosome. *Structure(Camb)*, 2004. 12: p. 1967-1975.
26. Shioi, S., Ose, T., Maenaka, K., Shiroishi, M., Abe, Y., Kohda, D., Katayama, T., and Ueda, T., Crystal structure of a biologically functional form of PriB from Escherichia coli reveals a potential single-stranded DNA-binding site. *Biochem. Res. Commun.*, 2005. 326: p. 766-776.
27. Huang, C.Y., Hsu, C.H., Sun, Y.J., Wu, H.N., and Hsiao, C.D., Complexed crystal structure of replication restart primosome protein PriB reveals a novel single-stranded DNA-binding mode. *Nucleic Acid Res.*, 2006. 34: p. 3878-3886.
28. Raghunathan, S., Kozlov, A.G., Lohman, T.M., and Waksman, G., Structure of the DNA binding domain of E. coli SSB bound to ssDNA. *Nat. Struct. Bio.*, 2000. 7: p. 648-652.
29. Lopper, M., et al., A hand-off mechanism for primosome assembly in replication restart. *Mol Cell*, 2007. 26 (6): p. 781-93.
30. F. Perrin, Polarisation de la lumière de fluorescence. *Vie moyenne des molécules dans l'etat excite*. *J. Phys. Radium*, 1926. 7: p. 390-401.
31. G. Weber, Rotational Brownian Motion and Polarization of the Fluorescence of Solutions. *Adv. Protein Chem.*, 1953. 8: p. 415-459.
32. J. R. Lakowicz, *Principles of Fluorescence Spectroscopy*, Plenum Press, New York, 1983.
33. Tina L. Mann and Ulrich J.Krull, Fluorescence polarization spectroscopy in protein analysis. *The Analyst*, 2003. 128: p. 313-317.
34. D. M. Jameson and T. L. Hazlett, in *Biophysical and Biochemical Aspects*

- of Fluorescence Spectroscopy, ed T. G. Dewey, Plenum Press, New York, 1991, ch. 4, pp. 105–133.
35. L. Lensun, T. A. Smith and M. L. Gee, Partial Denaturation of Silica-Adsorbed Bovine Serum Albumin Determined by Time-Resolved Evanescent Wave-Induced Fluorescence Spectroscopy. *Langmuir*, 2002. 18: p. 9924–9931.
36. W. Jin and J. D. Brennan, Properties and applications of proteins encapsulated within sol–gel derived materials. *Anal. Chim. Acta.*, 2002. 461: p. 1–36.
37. Kendrew, J. C.; G. Bodo, H. M. Dintzis, R. G. Parrish, H. Wyckoff, D. C. Phillips, A Three-Dimensional Model of the Myoglobin Molecule Obtained by X-Ray Analysis. *Nature*, 1958. 181 (4610): p. 662–666.
38. Table of entries in the PDB, arranged by experimental method.
39. http://en.wikipedia.org/wiki/File:X-ray_diffraction_pattern_3clpro.jpg
40. http://en.wikipedia.org/wiki/File:X_ray_diffraction.png
41. Hanging drop vapor diffusion crystallization, Hampton research.

APPENDICES

As described in chapter 1, primosome assembly in the *E. coli* DNA replication restart pathway is largely governed by weak interactions among primosome proteins that are strongly stimulated by the presence of DNA. Before I studied the DNA replication restart mechanism in *Neisseria gonorrhoeae*, I also worked to test the hypothesis that DnaB is actively recruited to repaired replication forks by direct protein:protein interaction between DnaT and DnaB/C complex in the PriA-PriB-DnaT pathway, and between PriC and the DnaB/C complex in the PriC pathway.

A-1

EXPRESSION OF *E. coli* DnaB

BL21(DE3) cells transformed with pET28b:dnaB were incubated at 37°C in Luria-Bertani medium supplemented with Kanamycin (LB/Kan medium) overnight. On the second day, the overnight culture was transferred into two separate 100 mL LB/Kan medium. I did not stop incubating the culture until OD₆₀₀ was greater than 0.4 when I set the time to 0. Then IPTG was added to a concentration of 0.5 mM to one of the cultures to induce while the other one remained untreated. I incubated both of them at 37°C and collected 500 µL samples at t=0, 1, 2, 3, 4 hours, respectively. To collect cells, the collected samples were centrifuged for 1 minute at 40,000 x g at room temperature. The supernatant was thrown away and the cells were stored at -20°C.

The cells were lysed with sample buffer and heated at 90°C for 9 minutes. I loaded 10 µL supernatant of every sample to a 10% SDS gel after I concentrated the samples for 2 minute at 40,000 x g at room temperature. The results show clear induction of DnaB protein due to IPTG (Figure 22). The bands got to their maximum density at 3 hours post-IPTG induction Based on this result, the best time to harvest cells for maximum protein overexpression is 2-3 hours after adding IPTG.

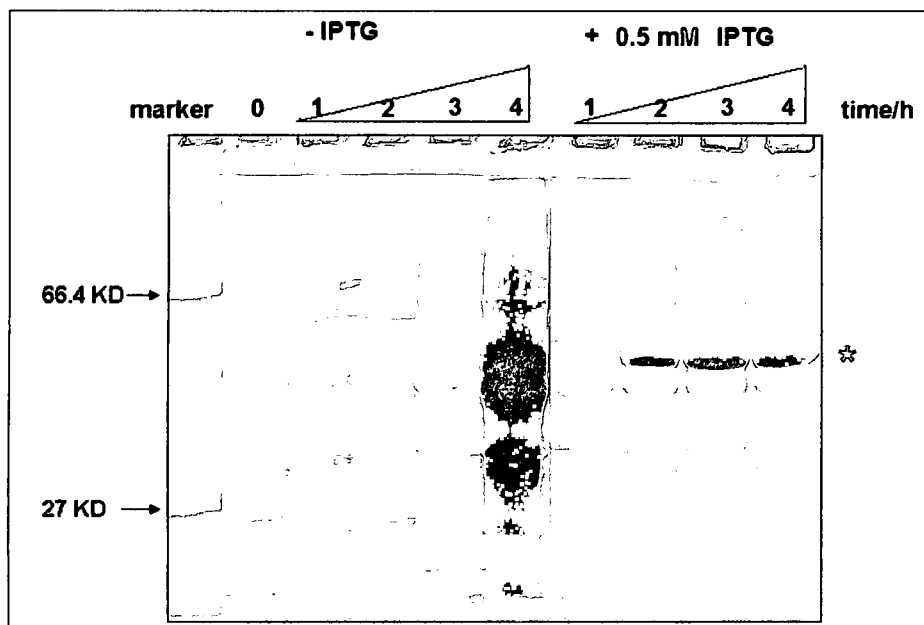


Figure 22. Timecourse of DnaB overexpression in *E. coli* cells. The concentration of IPTG is 0.5 mM; The growth temperature is 37°C; The molecular weight of *E.coli* DnaB is 52. 39 KD located as the star shows.

In order to get enough DnaB, BL21 (DE3) cells transformed with pET28b:dnaB were incubated at 37°C in 50 ml LB/Kan medium overnight. On the second day, the overnight culture was transferred into 1 L LB/Kan medium and incubated at 37°C. Protein expression was induced by the addition IPTG to 0.5 mM at the cells' OD₆₀₀ of 0.57. Then the cells were incubated for 3 hours before harvest by centrifugation for 25 min at 5500 x *g* at 4°C. The cells were stored at -80°C.

A-2

PURIFICATION OF *E.coli* DnaB

The cells were suspended in Lysis Buffer [10 mM Tris-HCl (pH 8.0), (v/v) 10% glycerol, 50 mM NaCl, 10 mM imidazole, 1 mM PMSF and 1 mM β -ME] at a v/w ratio of 3 ml/ gram cells. This process was followed by the addition of lysozyme to degrade intracellular debris, DNase I and RNase A to decompose DNA and RNA. The mixture turned viscous after the addition of lysozyme. But after incubated for about 15 minute with DNase I and RNase A, the mixture turned thin and runny. Insoluble debris was removed by centrifugation for 20 min at 40,000 x g at 4°C.

To eliminate contaminating proteins, 2 ml Ni-NTA slurry was added to the supernatant and incubated for 1 hour at 4°C in order to let the negatively charged protein bind to the Ni beads. The mixture was separated with a column. The beads binding with the protein that I want to get were blocked and the waste was in the flow through. The beads were washed with 25 ml Wash Buffer [10mM Tris-HCl (pH 8.0), (v/v) 10% glycerol, 50mM NaCl, 10mM imidazole and 1 mM β -ME] and then the protein was eluted by 15 mL Elution Buffer [10mM Tris-HCl (pH 8.0), (v/v) 10% glycerol, 50mM NaCl, 250mM imidazole and 1 mM β -ME]. I added 20 μ l thrombin to the elutant

and dialyzed the protein solution against Dialysis Buffer [10mM Tris-HCl (pH 8.0), (v/v) 10% glycerol, 50 mM NaCl and 1 mM β -ME]. Then, the protein solution was separated by a second nickel column. I added 0.5 ml Ni-NTA slurry to the mixture and incubated the mixture for 1 hour before I collected the flow through from a column which was further purified by an ion-exchange column. The type of IEC I used was QFF column that was washed by Buffer A [10mM Tris-HCl (pH 8.0), (v/v) 10% glycerol, 100 mM NaCl and 1 mM β -ME]. The protein then was eluted from the column with a linear gradient of Buffer B [10mM Tris-HCl (pH 8.0), (v/v) 10% glycerol, 1 M NaCl and 1 mM β -ME].

In the purification process, I collected 20 μ L samples for every step and check the results using a 10% SDS-PAGE (Figure 23). From the SDS-PAGE analysis, DnaB is mostly pure in lane 7. However, as time progressed, the amount of DnaB was reduced, while two smaller kinds of new proteins were produced. These are likely breakdown products of DnaB.

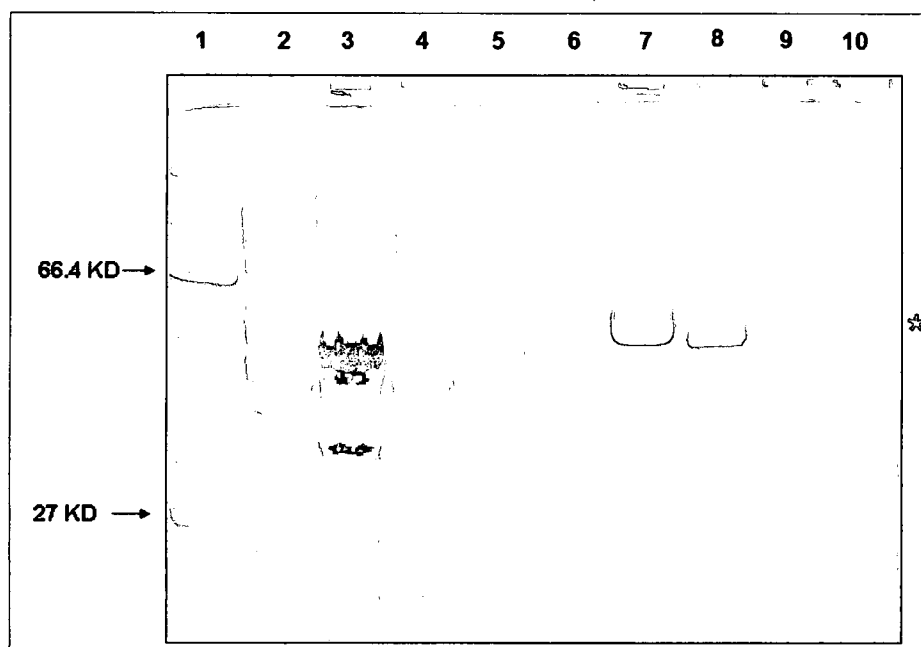


Figure 23. Purification process of *E.coli* DnaB. 1. protein marker; 2. lysate; 3. proteins in debris; 4. flowthrough of 1st Ni column; 5. early wash; 6. late wash; 7. elutant from 1st Ni column; 8. protein mixture with thrombin for 24 hours; 9. protein mixture with thrombin for 48 hours; 10. protein mixture after dialysis.

In order to get pure DnaB and avoid loss due to proteolysis, I changed the protocol of the purification of DnaB. After I got the elutant from the 1st Ni column, I ran a QFF column which was equilibrated and washed with the same Buffer A and Buffer B directly. The DnaB containing fractions detected by SDS-PAGE of the QFF column were collected and concentrated using a Centriprep-YM-10 concentrator to a volume less than 2 ml in the presence of 40 µl thrombin. 2 ml is the volume of S300 column (a size-exclusion column) that I used later on to do the last purification step. Thrombin can digest His-tags on DnaB and the products were separated by the S300 column which

was washed with S300 Buffer [10mM Tris-HCl(pH 8.5), (v/v) 10% glycerol, 500 mM NaCl and 1 mM β -ME]. I collected the DnaB containing fractions and concentrated the solutions with the same size concentrator overnight. The best concentration I got using this method was 1.90 g/L. The protein solution was store at -80°C.

This protocol solved the problems seen with the earlier attempt (Figure 24A). The band in lane 8 on the gel let me know that the protein solution is reasonably pure. During the concentration in the presence of thrombin, the concentration of DnaB was increased and some new smaller proteins which were separated by the S300 column were produced. The improvement of this method was that the DnaB was still there though the His-tags were cleaved off as the lane 9 showed. Here the molar mass of DnaB was lighter than the His-tagged structure.

Because of the different sizes, S300 column can separate DnaB from the contaminating components. The peak with a retention volume of 54.76 ml that is unique was the DnaB (Figure 24B). When I ran the same S300 column with different sized standard proteins, I got a plot of $\log (M.W.)$ versus their retention volume. The equation for their relationship was: $y = -0.0401x + 7.677$. I used this relationship, along with the retention volume of DnaB, to calculate the molecular weight of DnaB: 302.78KD This is almost six times of the molar mass of isomer of DnaB, indicating that DnaB is a hexamer under these conditions, as expected. The highlighted fractions were collected to analyze by SDS-PAGE (Figure 24C).

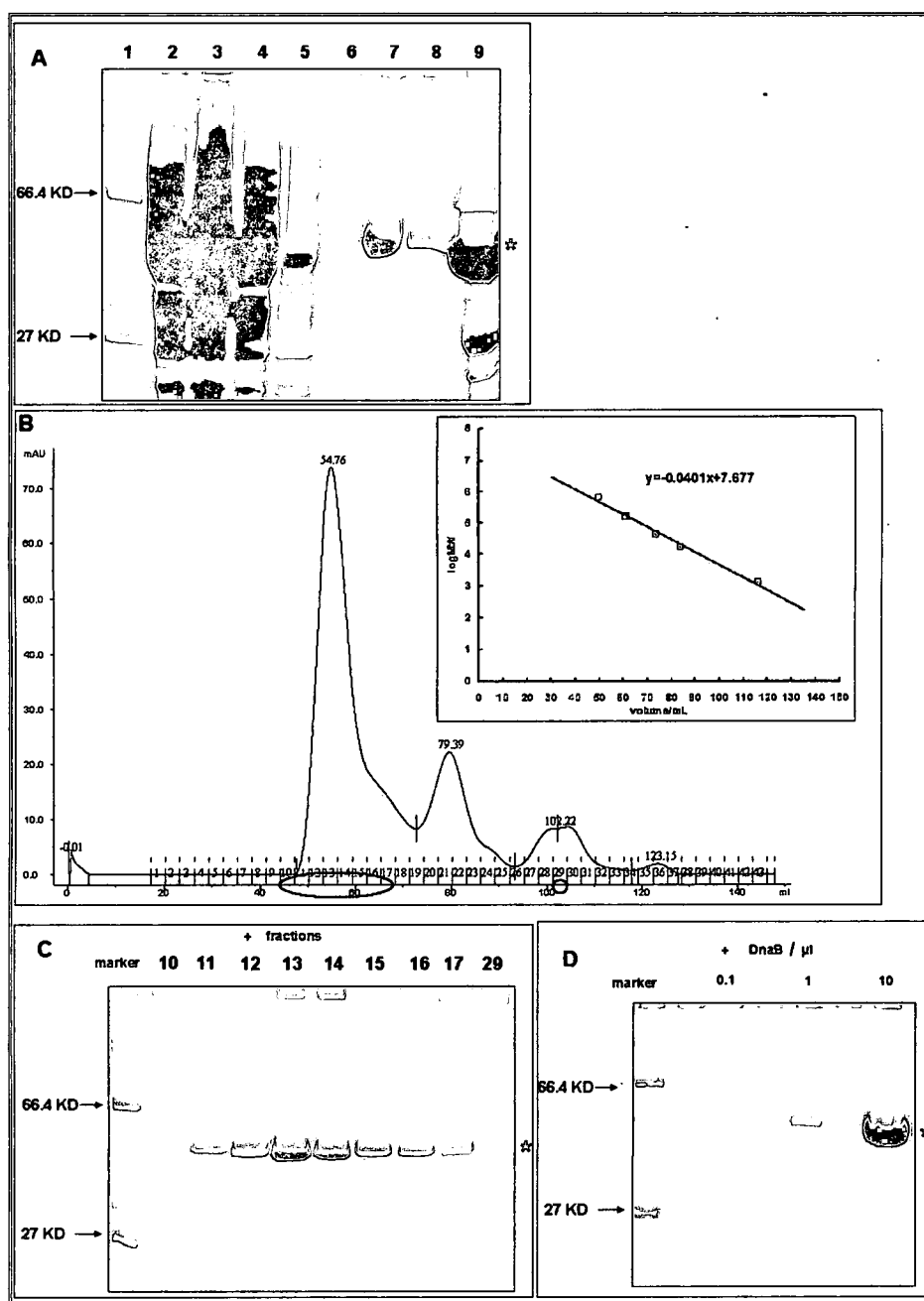


Figure 24. Results of DnaB purification process. A). 1. protein marker; 2. lysate; 3. proteins in debris; 4. flowthrough of 1st Ni column; 5. early wash; 6. late wash; 7. elutant from 1st Ni column; 8. protein mixture after IEC column; 9. protein mixture after Thrombin and concentration(which I loaded into the S300 column); B). IEC column spectrum. The highlighted fractions were collected. C). S300 column fractions on SDS-PAGE. D). Purity of DnaB solution.

The SDS-PAGE told me that the fractions: 12, 13, 14, and 15 were pure enough for me to collect. After concentration, I determined the concentration of DnaB using a UV-spectrophotometer. It was 1.90g/L with more than 95% purity as estimated by SDS-PAGE analysis (Figure 24D).

A-3

BINDING ABILITY OF *E. coli* DnaB

A-3-1 Interaction between *E. coli* DnaB and FITC-DnaT

In order to detect whether there is a physical interaction between DnaB and DnaT, I measured the fluorescence anisotropy of FITC-DnaT (26 μ M stock solution) with the presence and absence of *E. coli* DnaB. At first, I made all the solutions using FP Buffer A [10 mM Tris-HCl (pH 8), (v/v) 4% glycerol, 100 mM NaCl, 1 mM β -ME, and 0.1 g/L BSA]. FITC-DnaT was kept at a constant concentration of 10 nM, as I increased the amount of DnaB. If interaction exists, there should be a DnaB-dependent increase in fluorescence anisotropy. But the FP data that I got did not show this increase which means DnaB can not bind DnaT directly under this condition.

Because I was not sure if it was due to the buffer, I chose a different buffer called FP Buffer B [20 mM Tris-HCl (pH 8), (v/v) 15% glycerol, 150 mM NaCl, 1 mM β -ME, and 0.1 g/L BSA] to make all the solutions. However, the results did not show any evidence that DnaB can interact with DnaT.

Then I tried to find out which primosome protein can help them to interact with each other. Before I started the titration, I added PriA, PriB and ssDNA solution in FP Buffer A to FITC-DnaT solution. And the results showed that none of them facilitated the interaction. There was no DnaB-dependent increase in fluorescence anisotropy. As a result, I concluded that DnaB has neither direct interaction with DnaT nor an indirect interaction with DnaT through PriA, PriB and ssDNA.

A-3-2 Interaction between *E. coli* DnaB and FITC-PriB

Since the FP Buffers did not make any difference to the FP experiments for DnaB and FITC-DnaT, I went back to use FP Buffer A for all the experiments that were intent to detect the interactions between DnaB and FITC-PriB (130 μ M stock solution). Also, I kept FITC-PriB at a constant concentration of 10 nM when I titrated it using a series of difference concentrated DnaB solutions. If interaction exists, a DnaB-dependent increase in fluorescence anisotropy should be shown. But for this FP experiment, no increase appeared even I added DnaB to a high molar excess to FITC-PriB.

I added 2 μ l 100 μ M ssDNA solution to FITC-PriB solution before I started a new titration of the mixture. And later on, I tried two more sets of experiments. In the first set, I added 2 μ l of 100 μ M ssDNA solution and 2 μ l of 1 μ M PriA solution to FITC-PriB solution before I titrated them. And the second one, I added 2 μ l of 100 μ M ssDNA solution, 2 μ l of 1 μ M PriA solution and 1 μ l of 5 μ M DnaT solution to FITC-PriB solution before I titrated them. All the results of

these three trials did not show any increase in fluorescence anisotropy, indicating no interaction exists between DnaB and FITC-PriB even with the presence of PriA, DnaT and ssDNA.

To conclude, DnaB can not be loaded to the DNA replication restart site directly or with the presence of some other PriA, ssDNA , PriB and DnaT, which is not in contrast to our hypothesis that DnaB should be reloaded through DnaB/C complexes. So next step, I needed to get *E. coli* DnaC and test the effect of DnaC on DnaB binding ability.

A-4

EXPRESSION OF *E. coli* DnaC

BL21 (DE3) *E. coli* cells transformed with pET28b:dnaC were incubated at 37°C in LB/Kan medium overnight. On the second day, the overnight culture was transferred into two separate 100mL LB/Kan medium. I did not stop incubating the culture until OD₆₀₀ was greater than 0.4 when I set the time to 0. Then IPTG was added to a concentration of 0.5 mM to one of the cultures to induce, while the other one remained untreated. I incubated both of them at 37°C and collected 500 µL samples at t=0, 1, 2, 3, 4 hour respectively. To collect cells, the collected samples were centrifuged for 1 minute at 5500 x g at room temperature. The cells were stored at -20°C.

The cells was lysed with sample buffer and heated at 90°C for 9 minutes. I loaded 10 µL supernatant of every sample to a 10% SDS gel after I concentrated the samples for 2 minute at 15,000 rpm at room temperature. The gel showed that no obvious expression of DnaC (Figure 25A).

Next, I tried two different temperatures 25°C and 30°C and still used the LB/Kan medium and 0.5 mM IPTG to express *E. coli* DnaC. Other steps were the same with those at 37°C. The SDS-PAGE results indicated no expression

of DnaC under these conditions (Figure 26B and 25B and 25C). Because all of my trials in LB medium failed, I tried a new medium called 2YT medium. On the first day, I set up overnight culture with BL21 (DE3) cells transformed with pET28b:dnaC in 2YT/Kan medium at 37°C and I incubated the overnight culture in two 100 ml 3YT/Kan medium at 37°C on the second day. When the OD₆₀₀ got a value that was greater than 0.4, 0.1 mM and 0.5 mM IPTG were added to these two medium respectively. When I added IPTG to the medium, I set time to 0 and collected a 500 µL sample. All the other samples were collected every hour for four hours and prepared using the same method with *E. coli* DnaB. The results were also checked by SDS-PAGE (Figure 26). The results were still disappointing. No improvement was found in the new medium in the presence of different concentration of inducer IPTG.

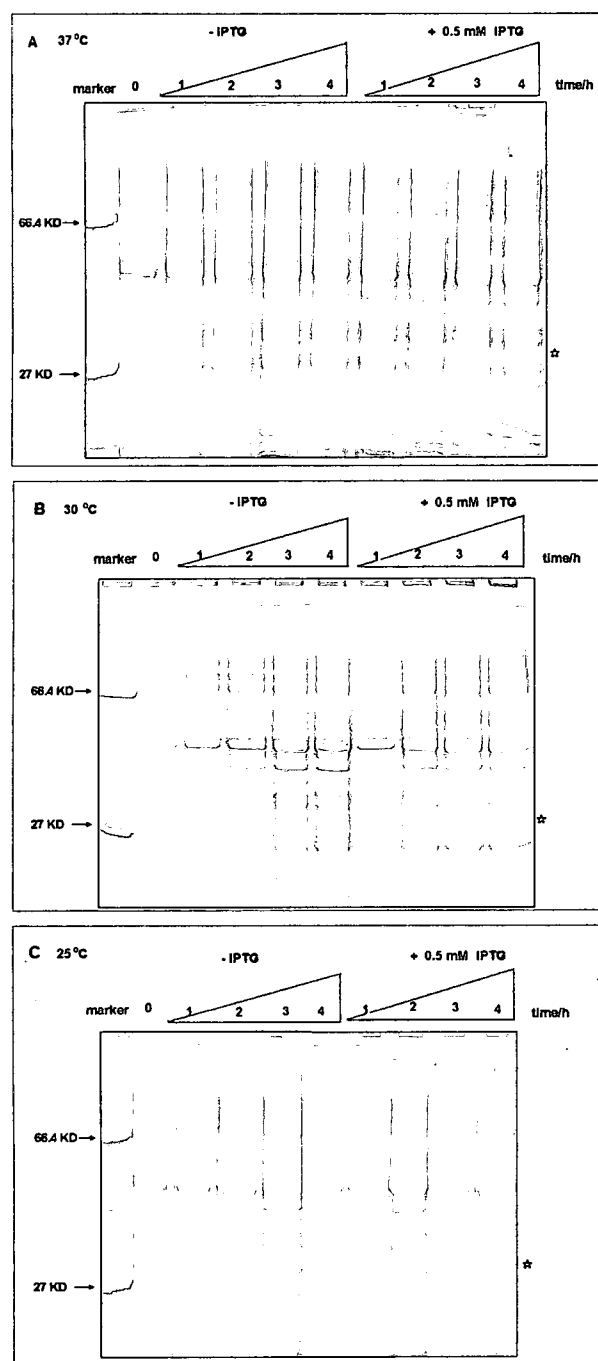


Figure 25. Overexpression of DnaC in LB/ Kan medium. A). Expression results of *E. coli* DnaC in LB/Kan medium with the inducer of 0.5 mM IPTG at 37°C; **B).** Expression results of *E.coli* DnaC in LB/Kan medium with the

inducer of 0.5 mM IPTG at 30°C. C). Expression results of *E.coli* DnaC in LB/Kan medium with the inducer of 0.5 mM IPTG at 25°C.

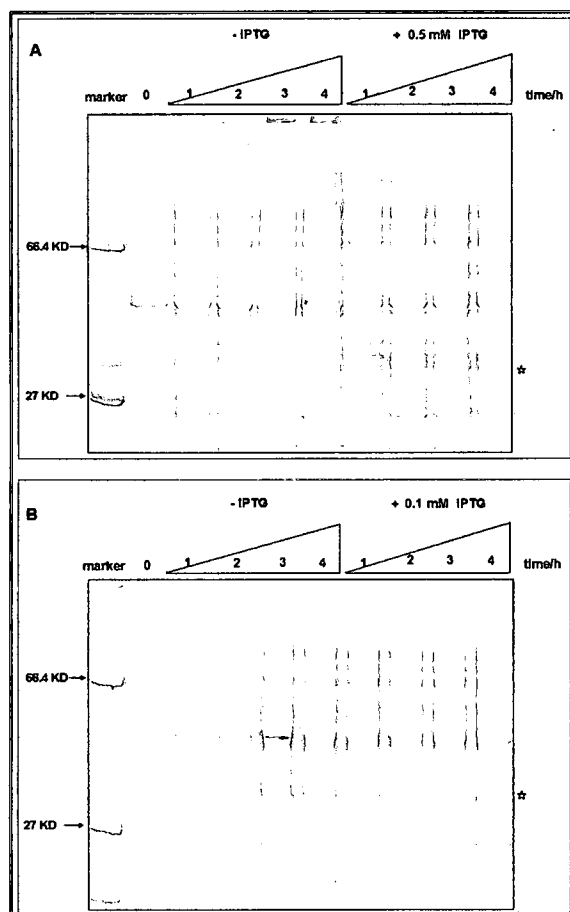


Figure 26. **Overexpression of DnaC in 2YT/Kan medium.** A). Expression results of *E.coli* DnaC in 2YT/Kan medium with the inducer of 0.5 mM IPTG at 37°C. B). Expression results of *E.coli* DnaC in 2YT/Kan medium with the inducer of 0.1 mM IPTG at 37°C.

I also tested overexpression of DnaC in the presence of 1% glucose to inhibit basal expression of DnaC during the growth phase of the cultures when overexpression of DnaC might be toxic to the cells. Unfortunately, addition of

R002594687

1% glucose to the culture medium did not result in improved expression of DnaC (Figure 27).

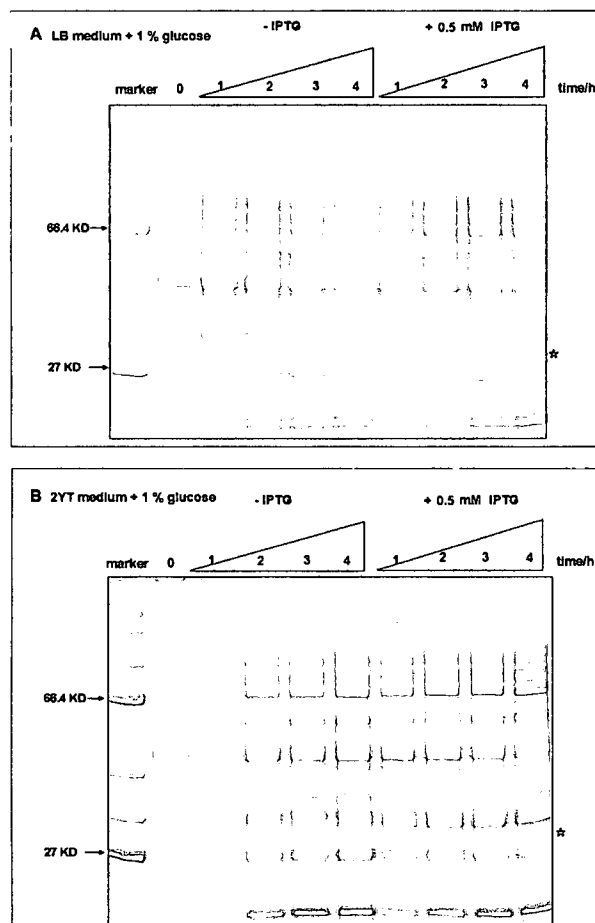


Figure 27. Overexpression of DnaC in the presence of glucose. A). Expression results of *E.coli* DnaC in LB/Kan/glucose medium with the inducer of 0.5 mM IPTG. **B).** Expression of *E.coli* DnaC results in 2YT/Kan/glucose medium with the inducer of 0.5 mM.

From these experiments, I conclude that DnaC can not be overexpressed using the most commonly used methods described here.